Magnetic imaging by LEEM, X-PEEM, X-ray microscopy, and X-ray holography

Wolfgang Kuch, Freie Universität Berlin

<u>basics:</u>

- x-ray absorption detection schemes
- cathode lens: working principle, resolution
- photoelectron emission microscopy (PEEM)
- low energy electron microscopy (LEEM)
- magnetic transmission x-ray microscopy (M-TXM)

<u>advanced chapters:</u>

- imaging by magnetic linear dichroism
- electron energy filtering in PEEM
- time-resolved magnetic imaging
- aberration correction
- imaging x-ray holography

Layered magnetic systems

magnetic read head

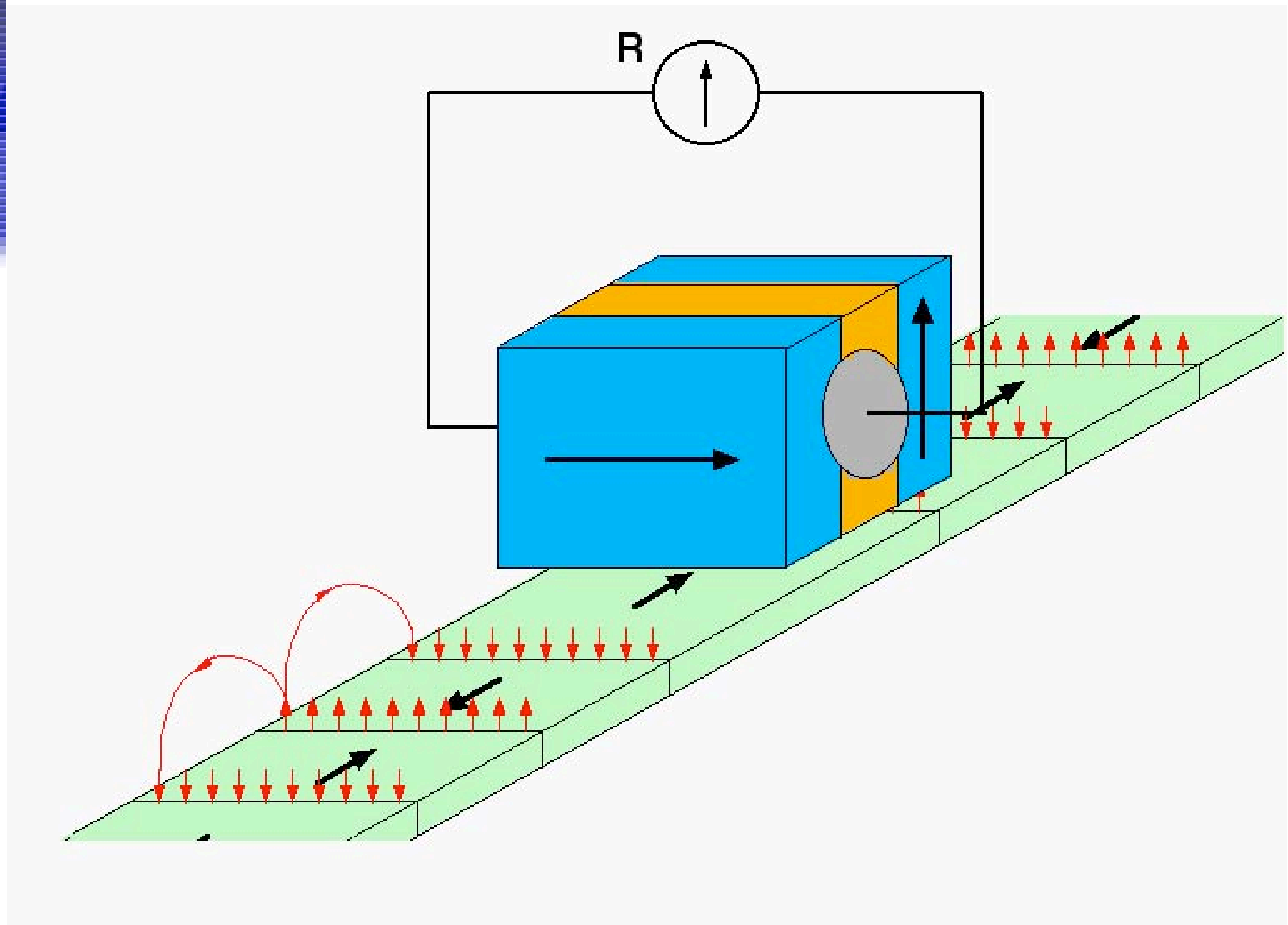

Layered magnetic systems

magnetic RAM

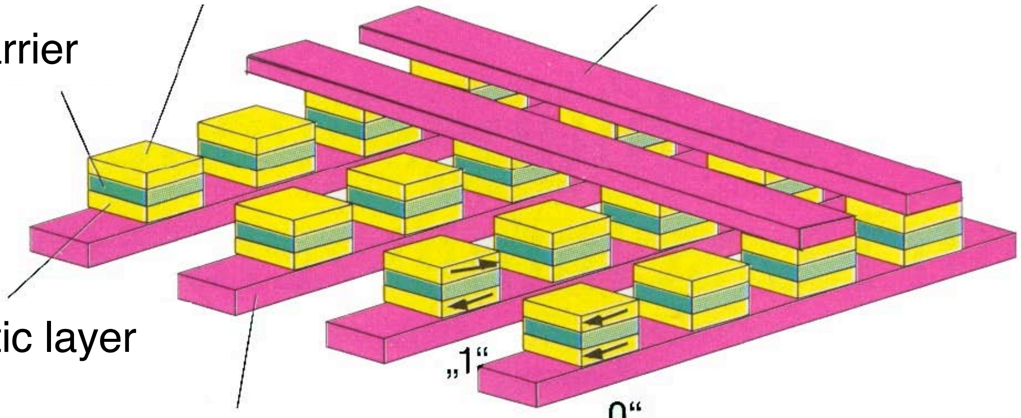

G. Reiss et al., Phys. Bl. 54 (1998) 339

Layered magnetic systems

giant magnetoresistance (GMR)

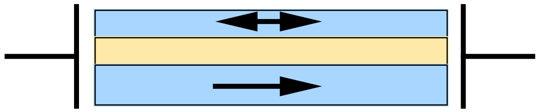

metallic conductivity

(sensor, hard disk read head)

tunnel magnetoresistance (TMR)

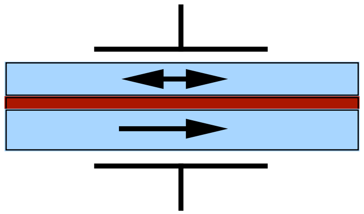

tunneling current

(sensor, magnetic RAM)

spin torque transfer

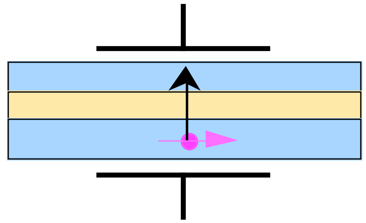

momentum transfer by
spin polarised e^-
(fast switching)

spin transistor

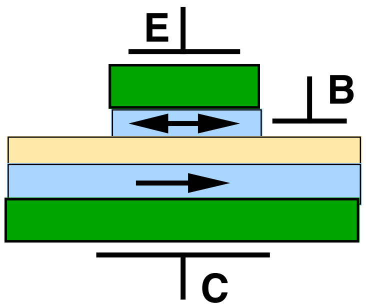

spin transistor with tunnel barrier

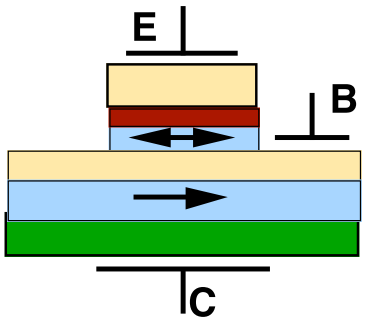

(logical devices, taking advantage of charge and spin)

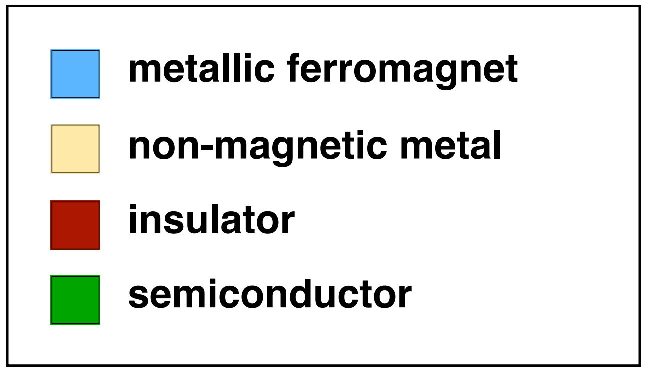

Layer-resolved information from XMCD

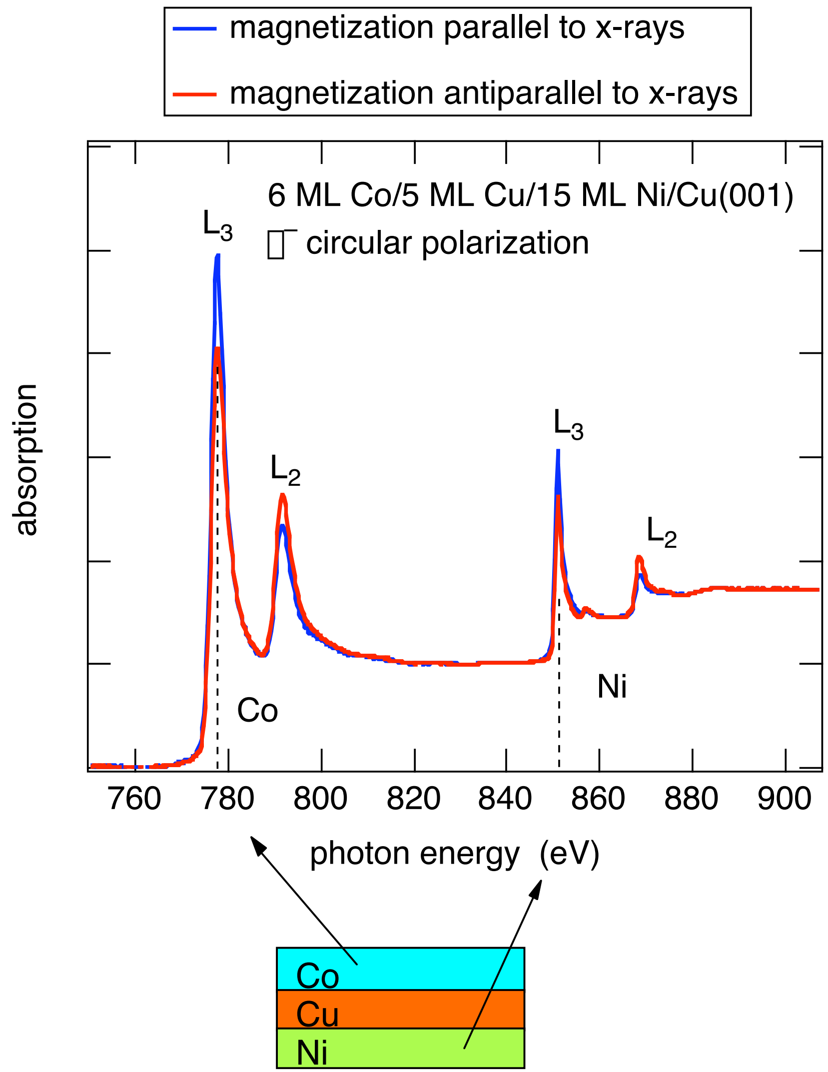

Synchrotron radiation needed

Detection methods for x-ray absorption

1.) “Total electron yield”

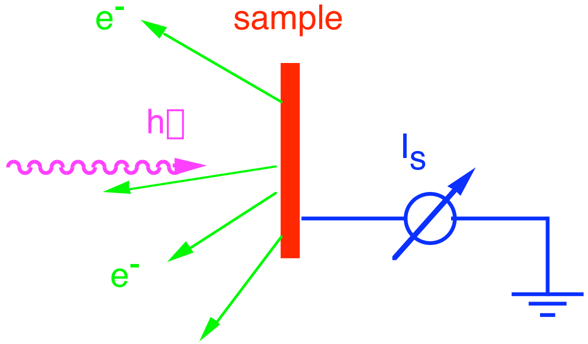

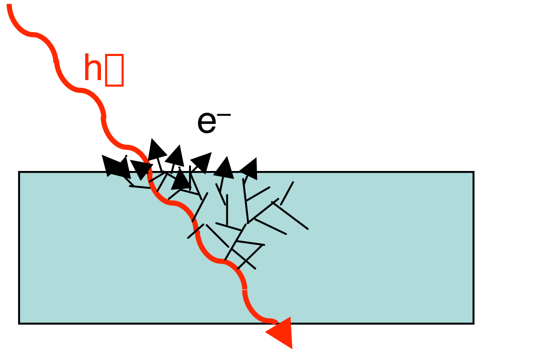

– ≈ proportional absorption
– surface sensitive (λ ≈ 20 Å)

2.) Transmission

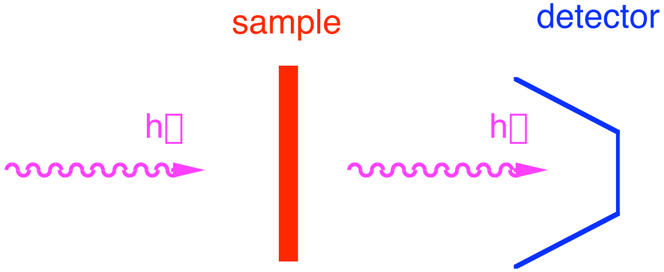

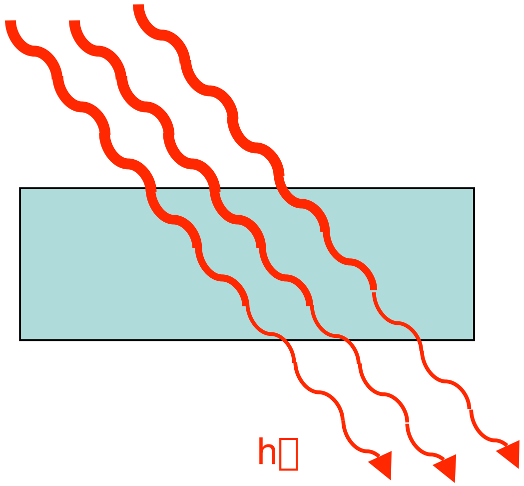

– real “absorption”
– only very thin substrates

Imaging the x-ray absorption

1.) "Total electron yield"

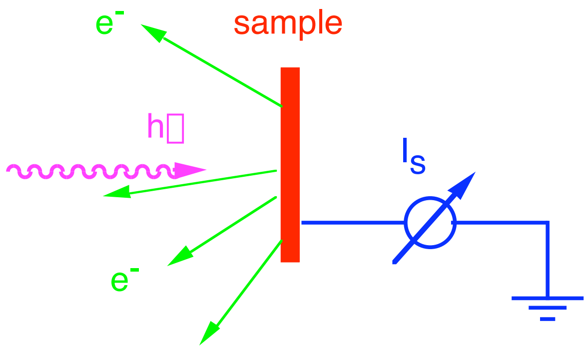

- ≈ proportional absorption
- surface sensitive (λ ≈ 20 Å)

2.) Transmission

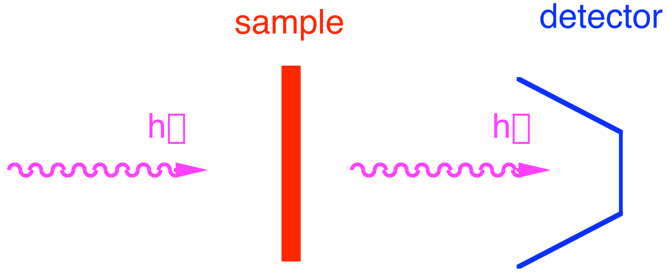

- real "absorption"
- only very thin substrates

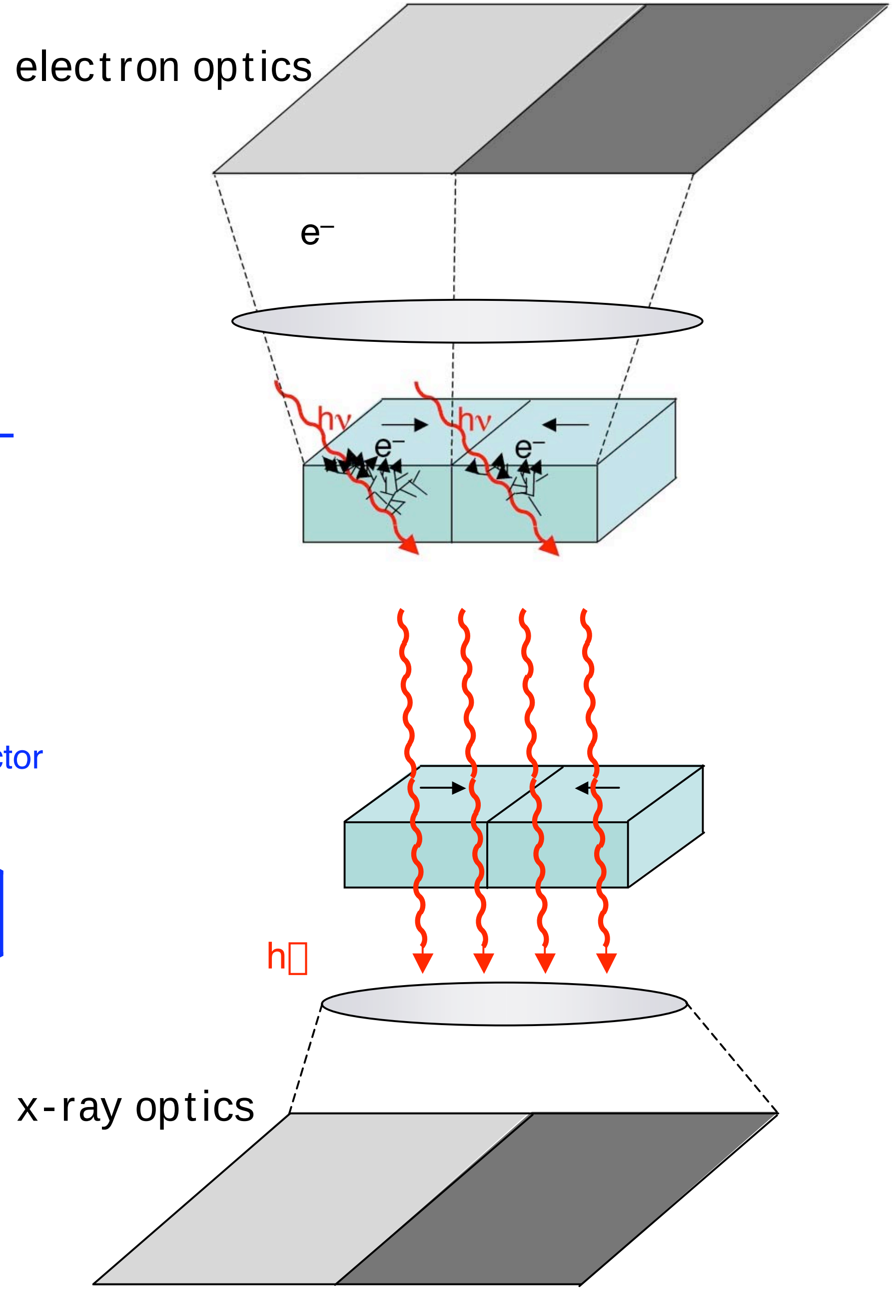

Optical imaging: Ideal lens

$$\frac{1}{f} = \frac{1}{p} + \frac{1}{q}$$

$$\frac{P}{Q} = \frac{p}{q}$$

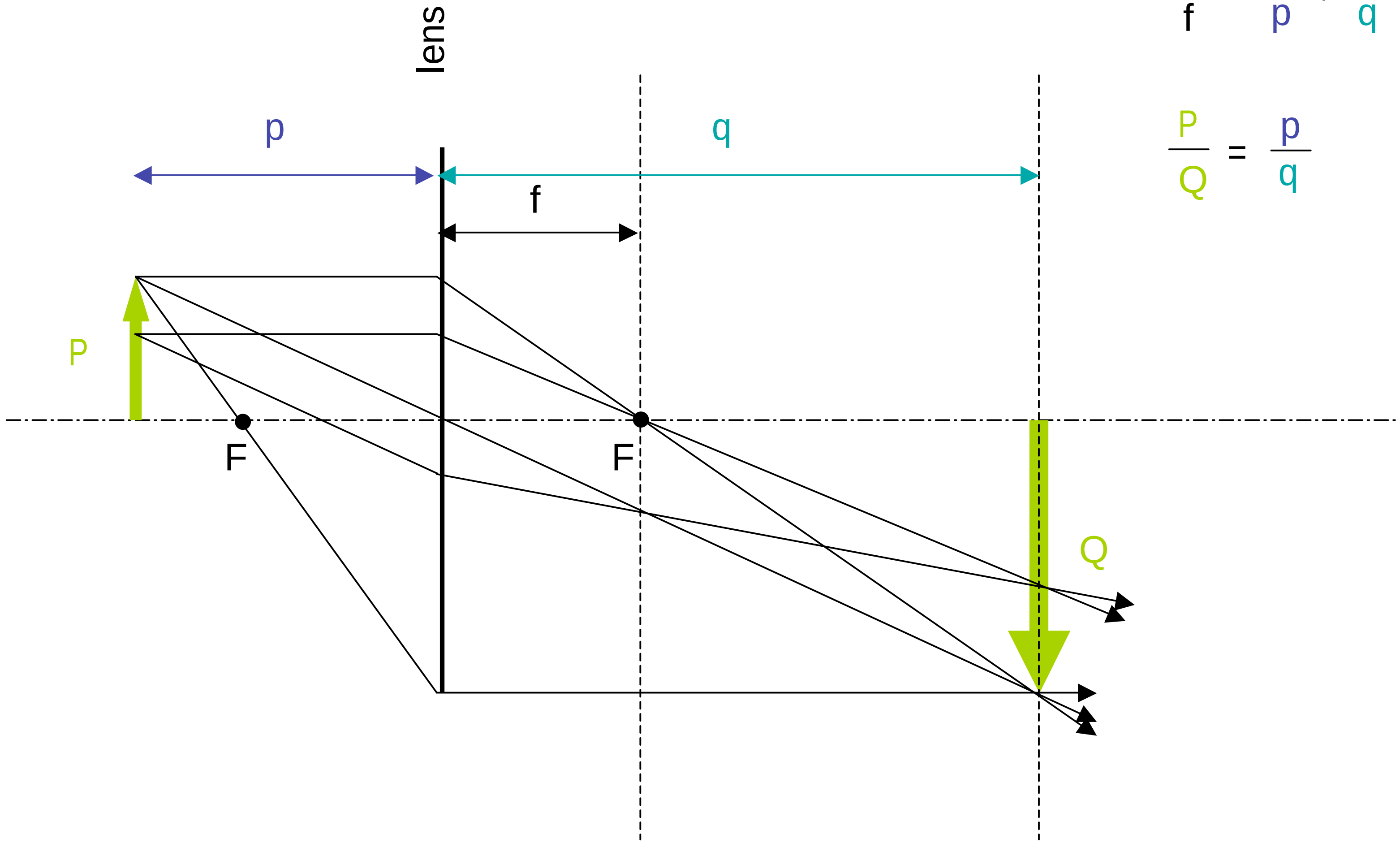

focal plane:
beams starting under identical angles meet

image plane:
beams starting at same position meet

Cathode lens for electron emission microscopy

electrostatic
triode lens

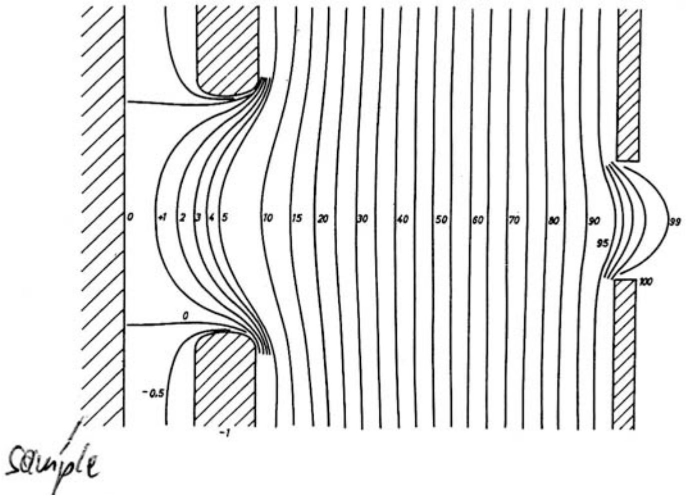

H. Seiler, “Abbildung von Oberflächen”, Bibliographisches Institut, Mannheim (1968)

electrostatic
tetrode lens

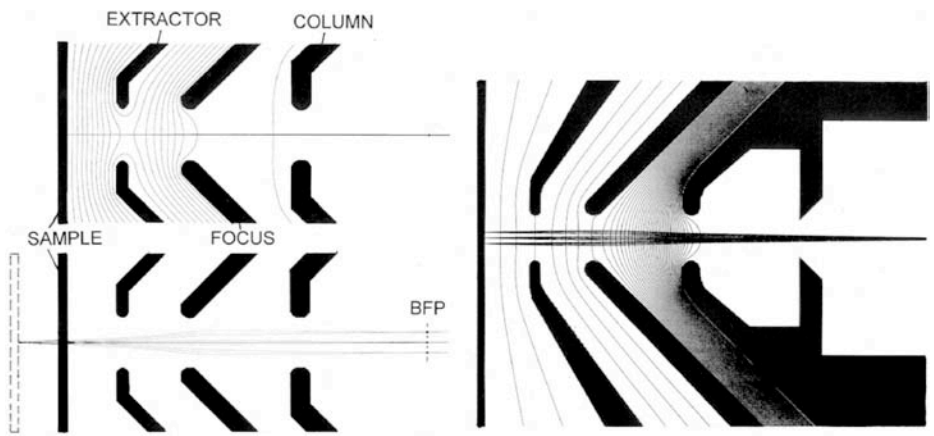

G. Schönhense, J. Phys.: Cond. Matt. 11 (1999) 9517

Cathode lens for electron emission microscopy

electrostatic tetrode lens

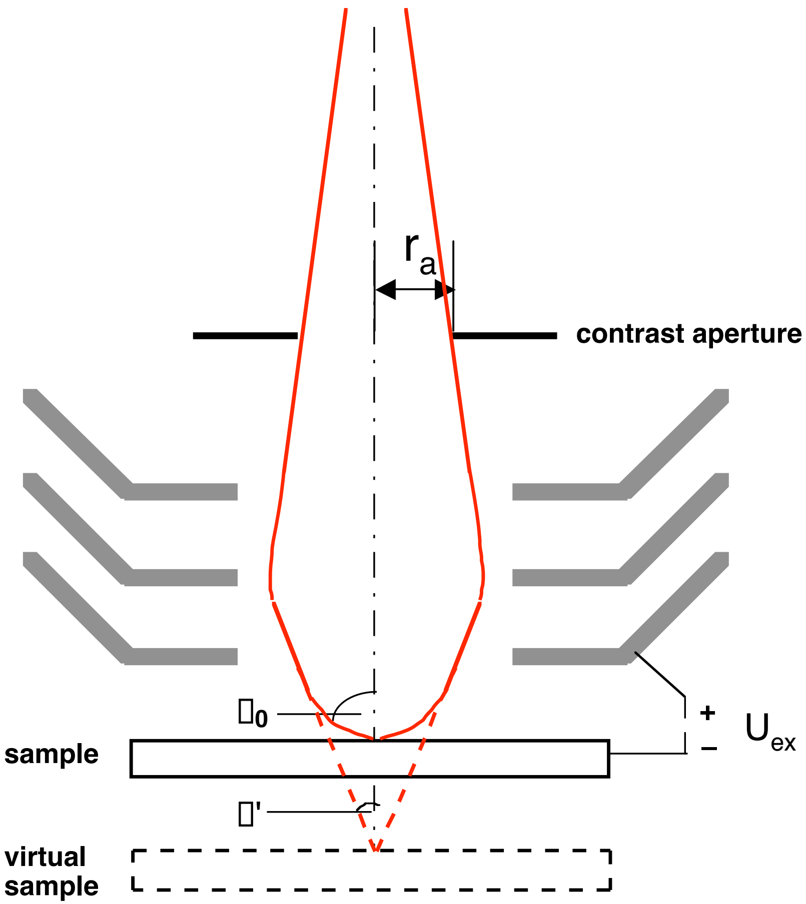

sample is part of optical system

real starting angle α_0

virtual starting angle α'

$$k_{||} = k \sin\alpha_0 = k' \sin\alpha'$$

$$k = \frac{\sqrt{2mE_0}}{\hbar} \qquad k' = \frac{\sqrt{2m(E_0 + eU_{ex})}}{\hbar}$$

$$\Rightarrow \quad \frac{\sin\alpha_0}{\sin\alpha'} = \sqrt{\frac{eU_{ex}}{E_0} + 1}$$

$$\boxed{\frac{\alpha_0}{\alpha'} \approx \sqrt{\frac{eU_{ex}}{E_0}}}$$

accepted solid angle $\Delta\Omega \ \mu \ \frac{1}{E_0}$

Photoelectron spectrum using a cathode lens

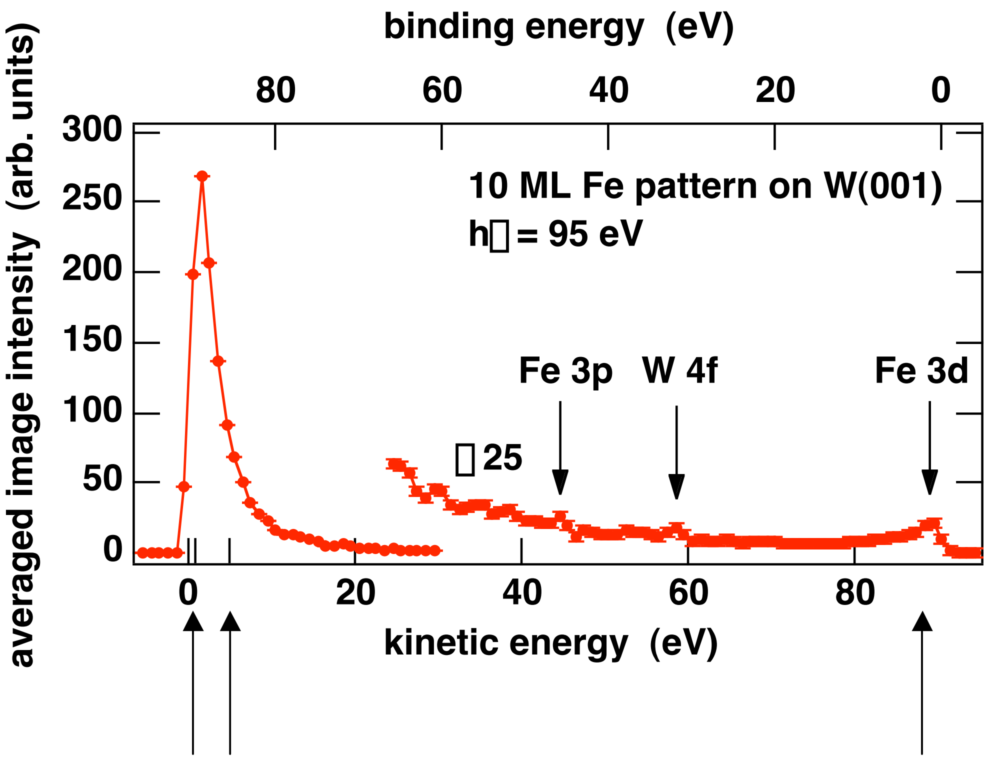

α_0 : 18° 8° 2°

$U_{ex} = 3.4$ keV

$2r_a = 150$ μm

$$\frac{\alpha_0}{\Delta\alpha} \approx \sqrt{\frac{eU_{ex}}{E_0}}$$

accepted solid angle $\Delta\Omega \propto \frac{1}{E_0}$

Aberrations in optical imaging

spherical aberration

$$d_s = \frac{1}{2} C_s \alpha^3$$

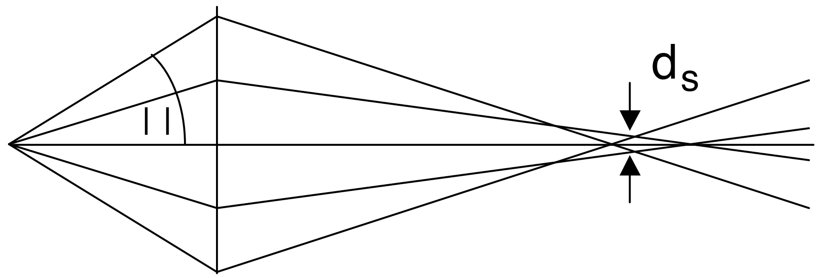

chromatic aberration

$$d_c = C_c \frac{\Delta E}{E} \alpha$$

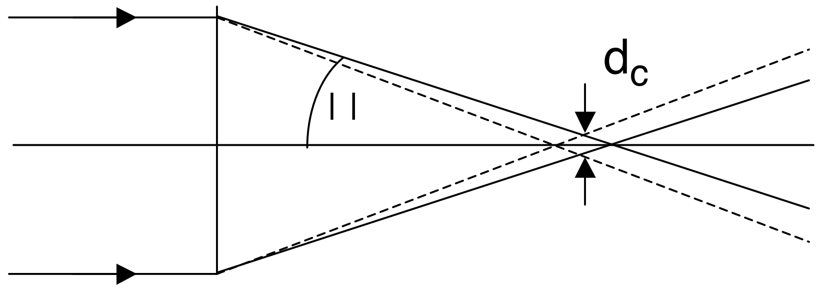

diffraction error

$$d_D \approx \frac{1}{2} \frac{\lambda}{\alpha}$$

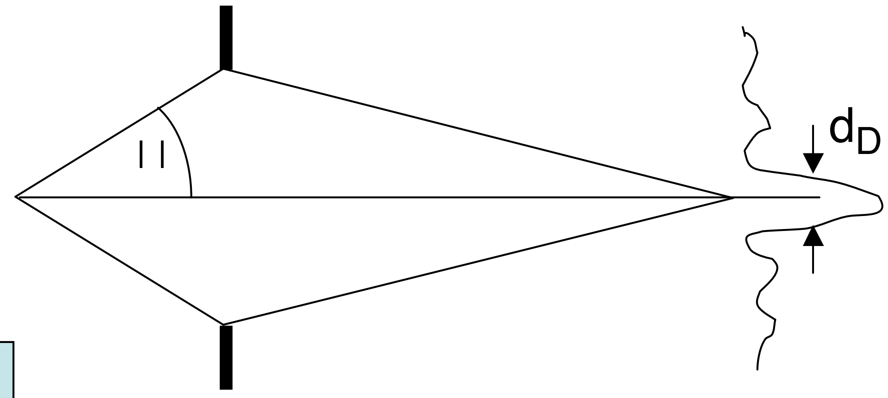

	C_s	C_c
magnetic	$\approx f$	$\approx f$
electrostatic	$\approx 10f$	$\approx 4f$

Resolution limit

spherical aberration

$$d_s = \frac{1}{2} C_s \square^3$$

chromatic aberration

$$d_c = C_c \frac{\square E}{E} \square$$

diffraction error

$$d_D \square \frac{1}{2} \frac{\square}{\square}$$

$\square\ \mu\ r_A$ $\qquad$ $d = \sqrt{d_s^2 + d_c^2 + d_D^2}$

theoretical resolution

(magnetic triode, 25 kV/3 mm, E = 2.5 eV, $\square$E = 0.25 eV)

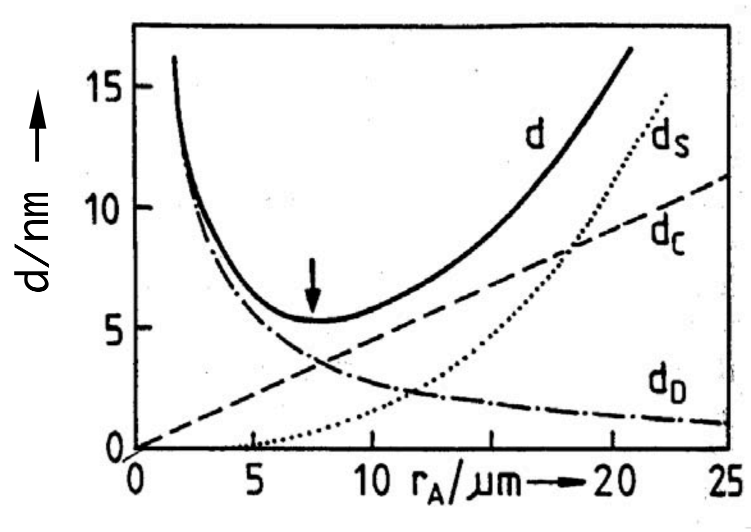

E. Bauer, Surf. Rev. Lett. 5 (1998) 1275

Cathode lens: Flat samples required

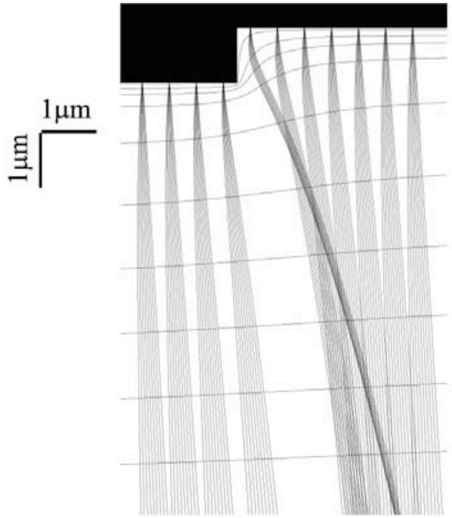

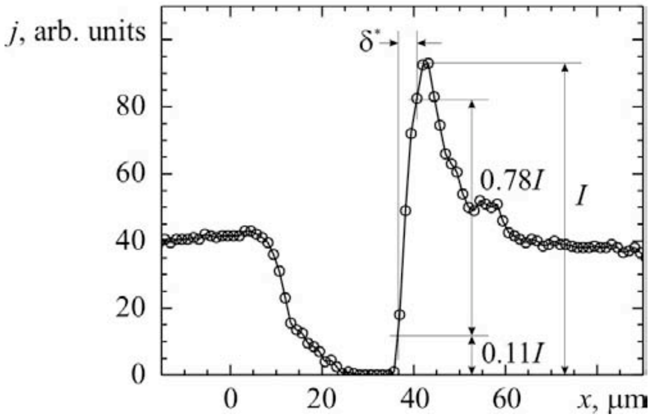

S. A. Nepijko et al., Ann. Phys. 9 (2000) 441

Electrostatic photoelectron emission microscope (PEEM)

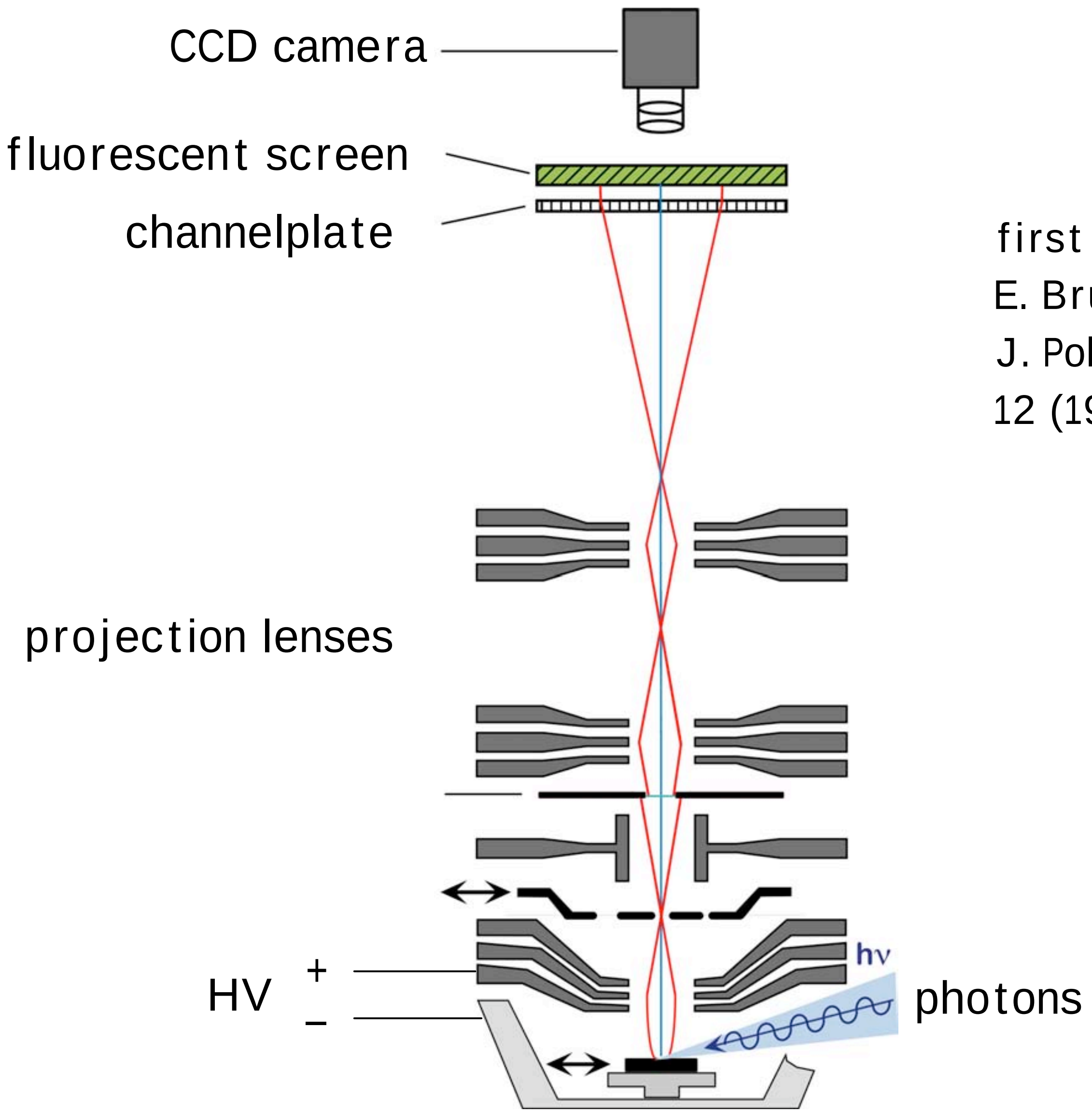

first use:
E. Brüche, Z. Phys. 86 (1933) 448;
J. Pohl, Zeitschr. f. techn. Physik 12 (1934) 579

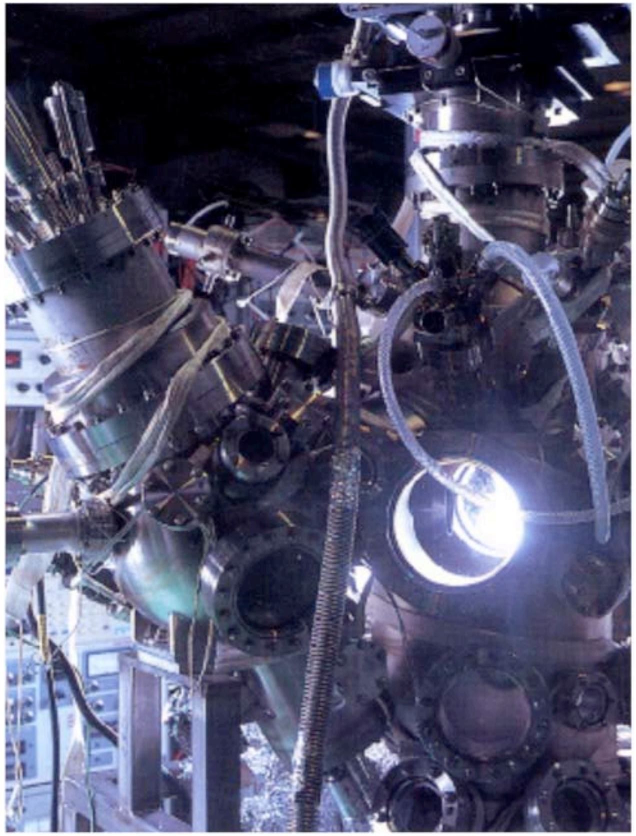

PEEM contrast: work function

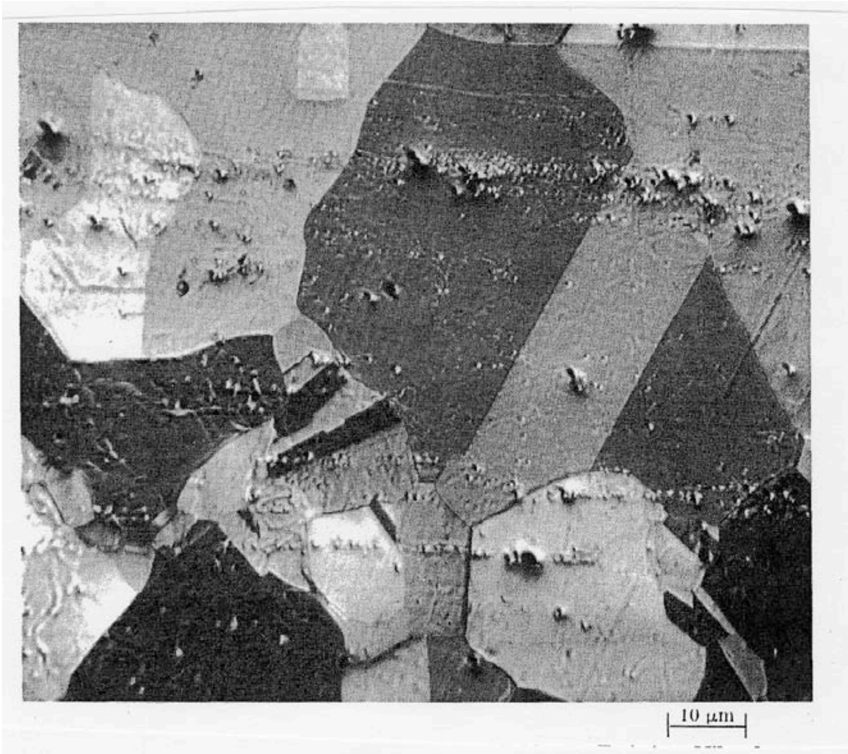

work function contrast
from coarse-grained Au

Hg lamp ($h\nu$ = 4.9 eV)

H. Seiler, “Abbildung von Oberflächen”, Bibliographisches Institut, Mannheim (1968)

PEEM contrast: topographic

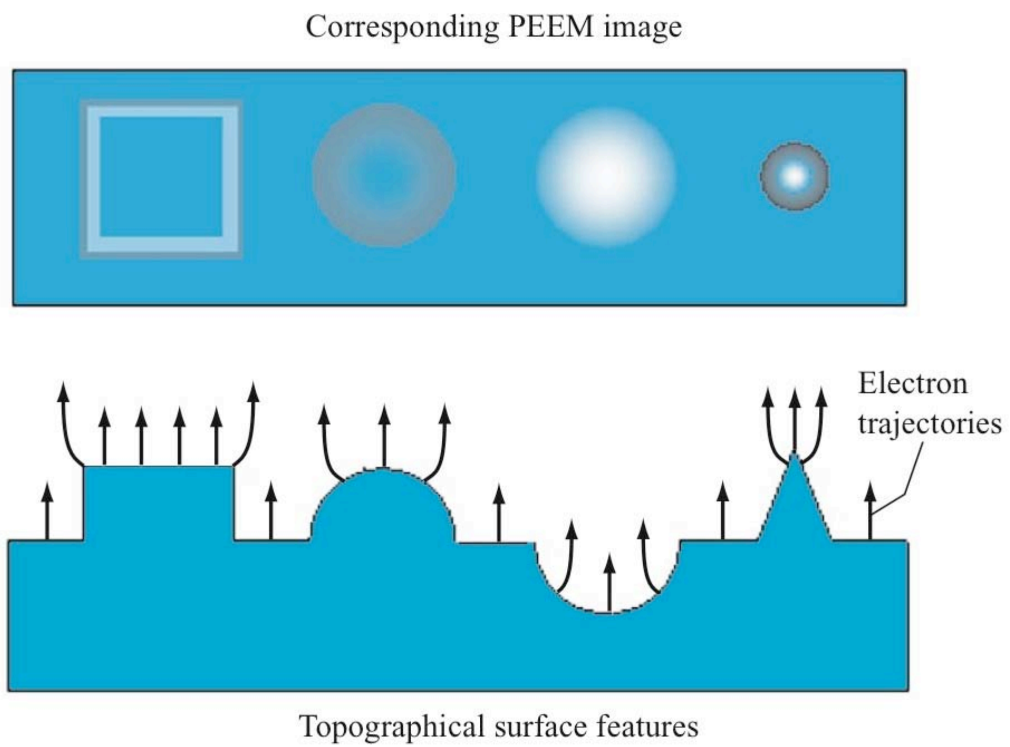

J. Stöhr and S. Anders, IBM J. Res. Develop. 44 (2000) 535

PEEM contrast: spectroscopic

elemental

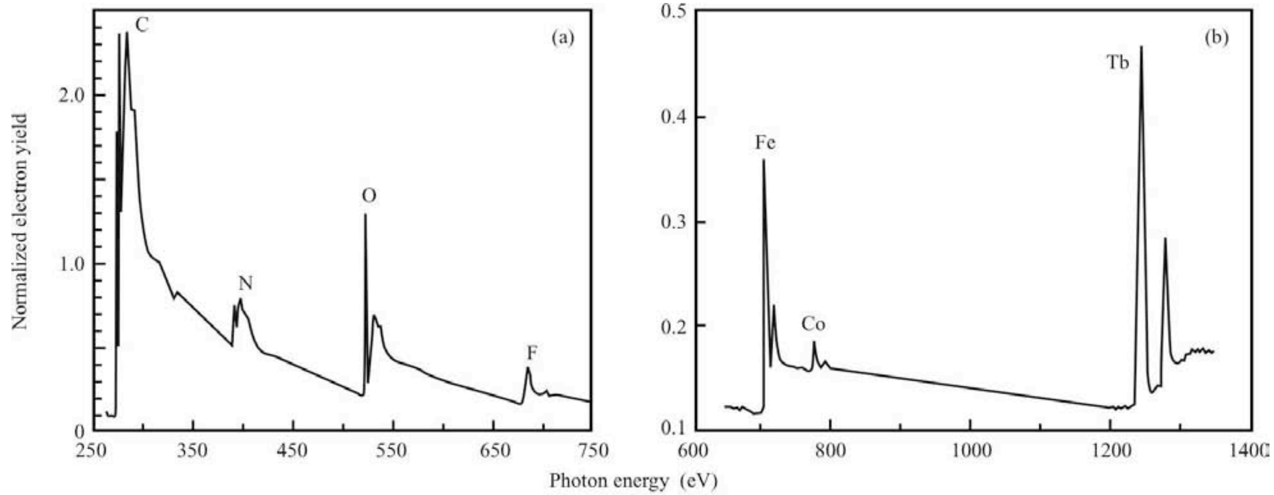

chemical

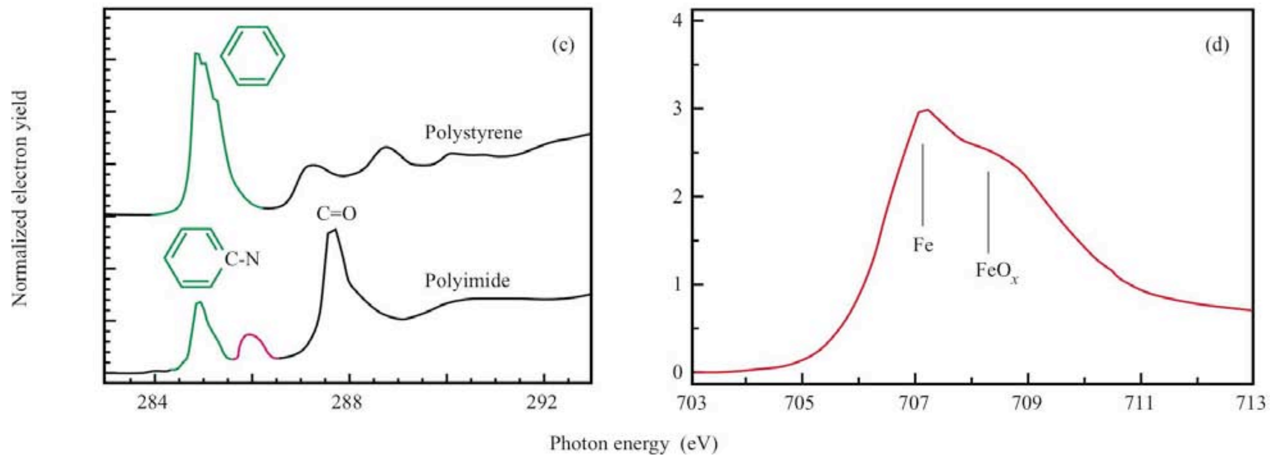

J. Stöhr and S. Anders, IBM J. Res. Develop. 44 (2000) 535

PEEM contrast: spectroscopic

magnetic

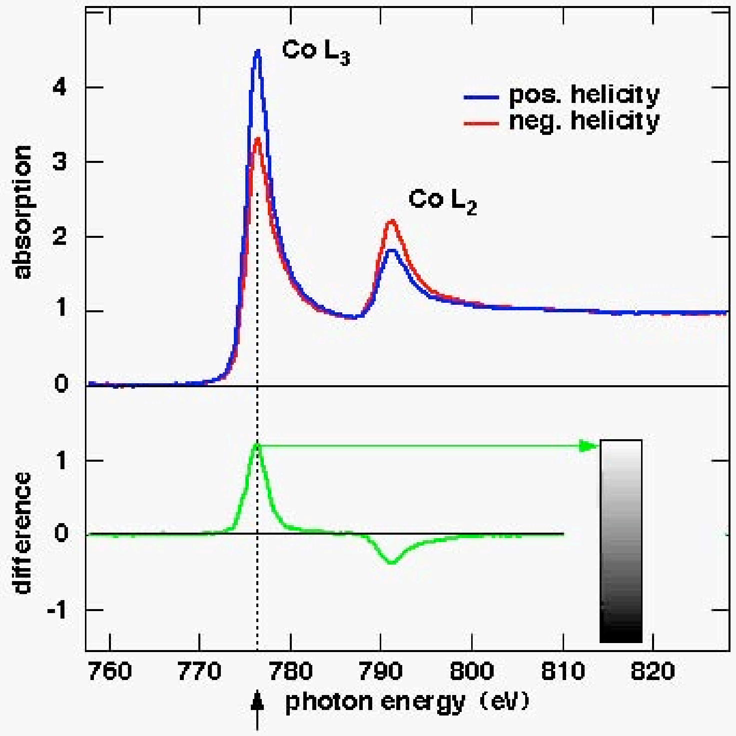

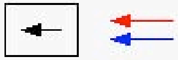

XMCD-PEEM: separate magnetic and topographic information

$I(\sigma^+)$

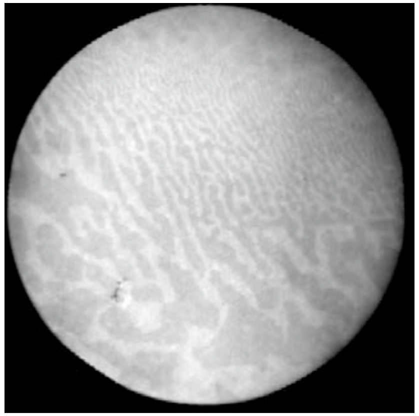

$I(\sigma^-)$

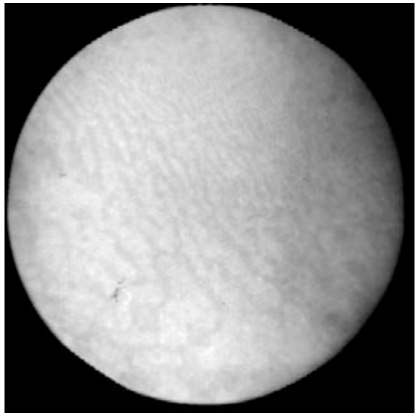

Co/Ni/Cu(001)

$$\frac{I(\sigma^+) - I(\sigma^-)}{I(\sigma^+) + I(\sigma^-)}$$

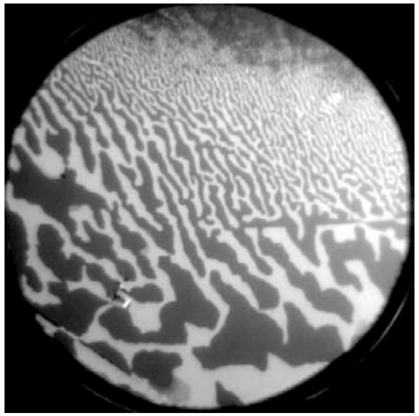

20 μm

W. Kuch, FUB,
K. Fukumoto, J. Wang, MPI-MSP,
C. Quitmann, F. Nolting, T. Ramsvik, PSI-SLS,
unpublished.

XMCD-PEEM: vectorial information by variation of incidence direction

Co L_3

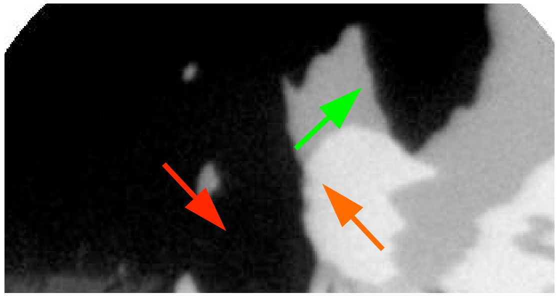

Co/FeMn/Cu(001)

hν

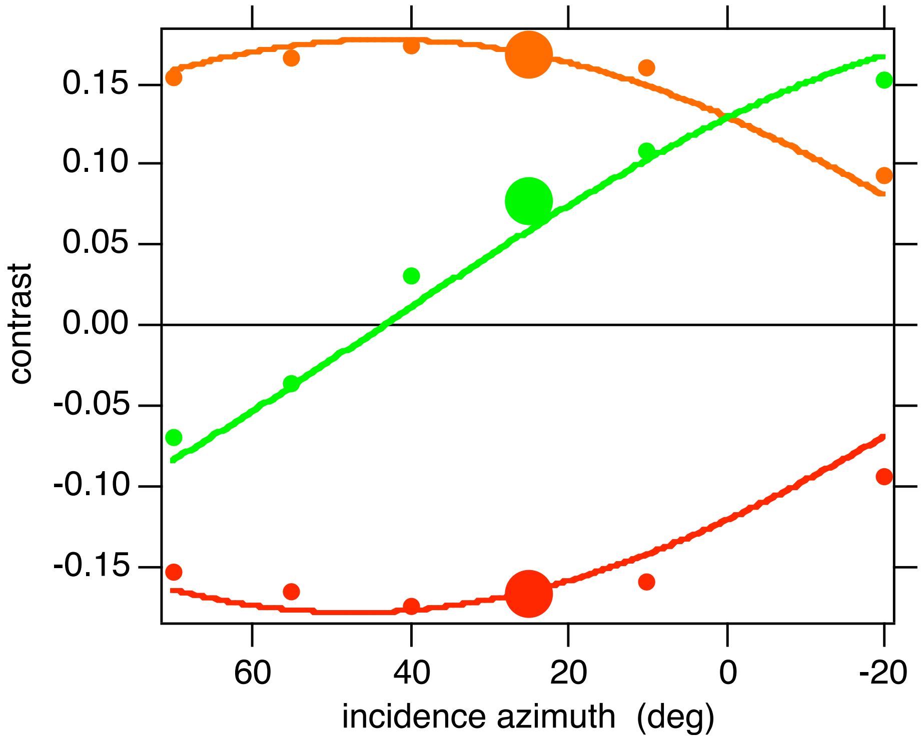

W. Kuch, F. Offi, L. I. Chelaru, J. Wang, K. Fukumoto, M. Kotsugi, MPI-MSP (unpublished)

Layer-resolved magnetic images

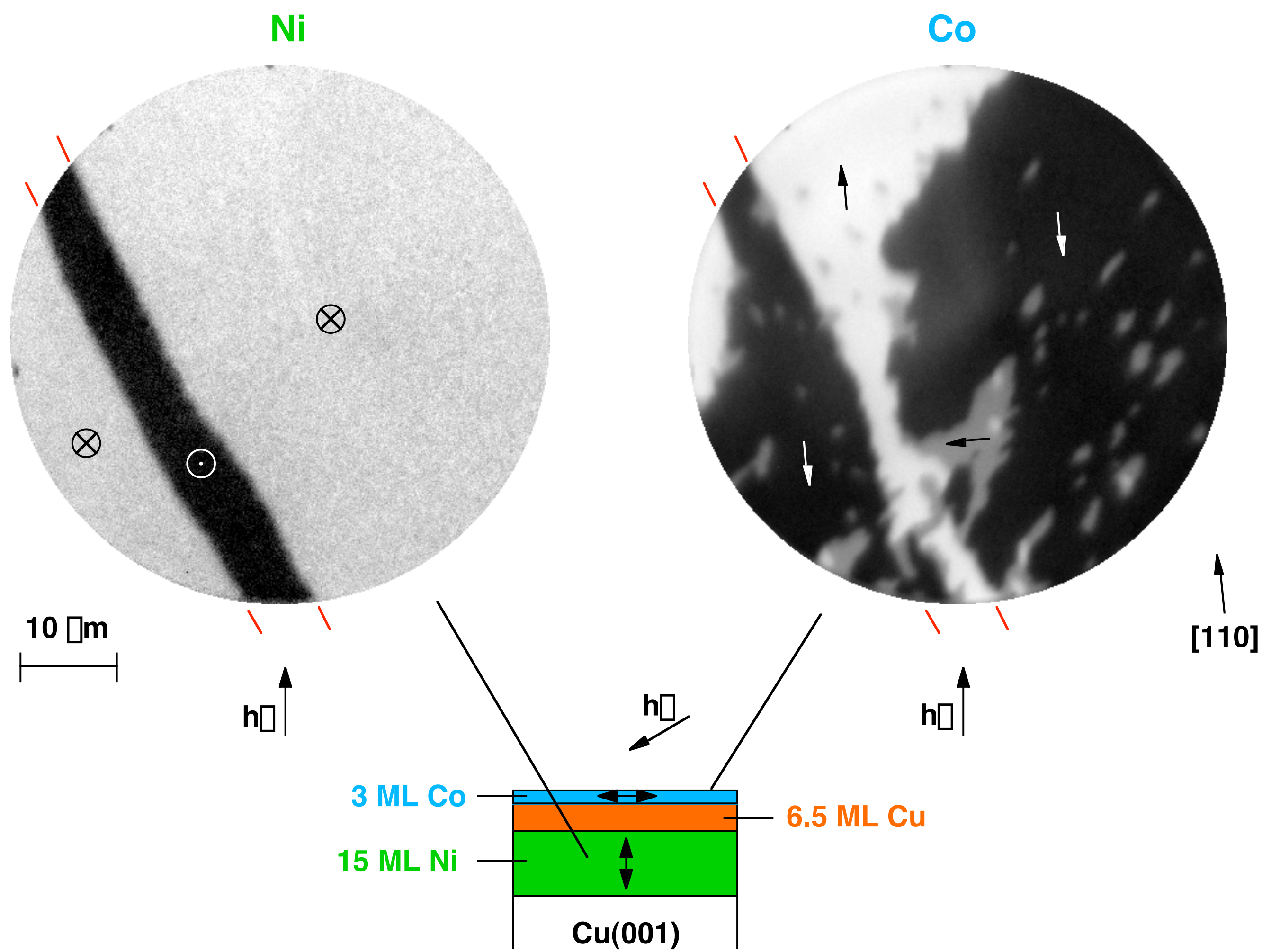

Attenuation of secondary electron yield

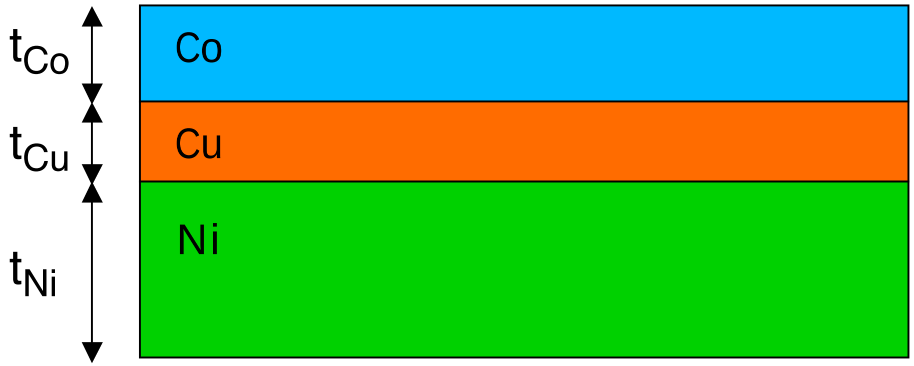

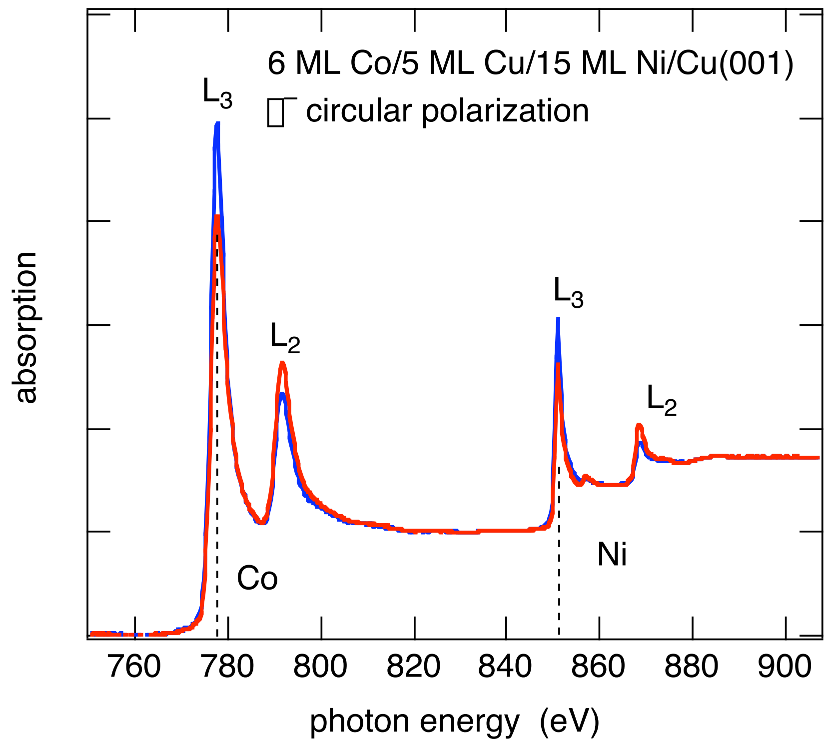

$$I_{Ni} \propto (1 - e^{-t_{Ni}/\lambda_{Ni}})\, e^{-t_{Cu}/\lambda_{Cu}}\, e^{-t_{Co}/\lambda_{Co}}$$

$\lambda \approx 2$ nm

Attenuation of secondary electron yield

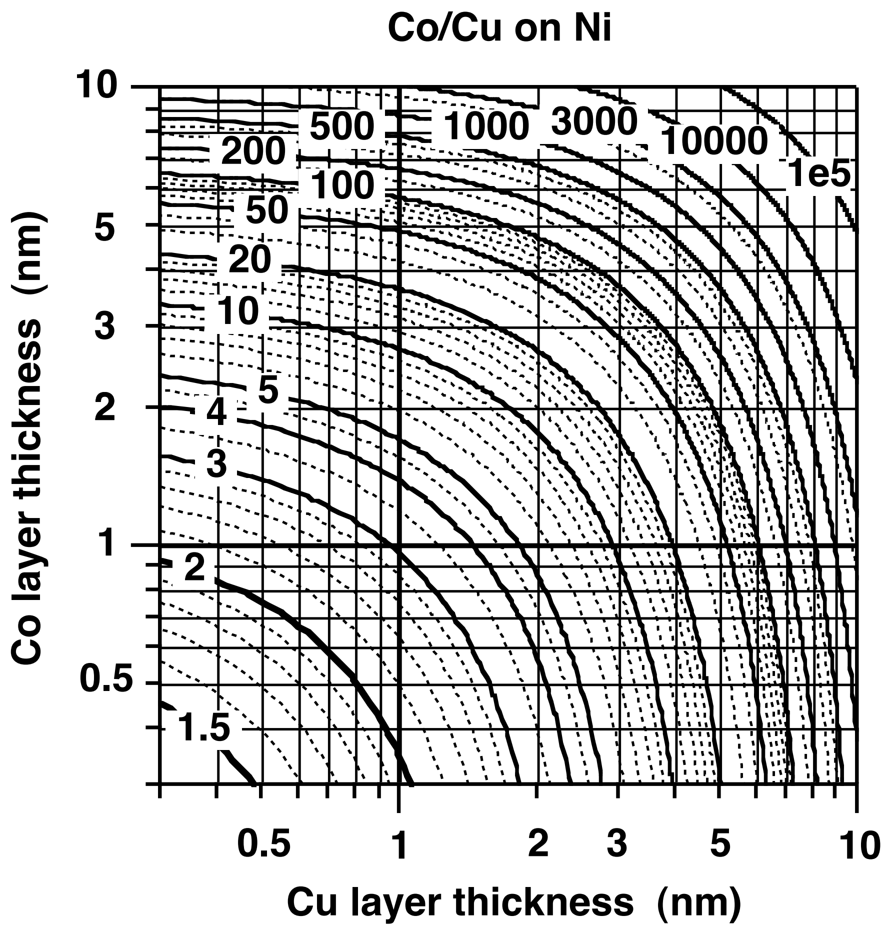

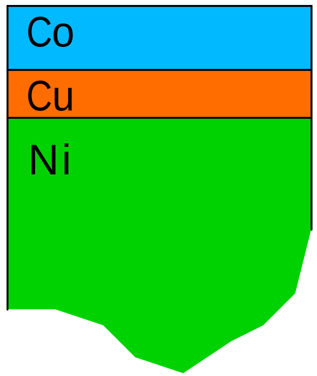

exposure time for same noise level as without overlayers

XMCD-PEEM: layer-resolved magnetic imaging

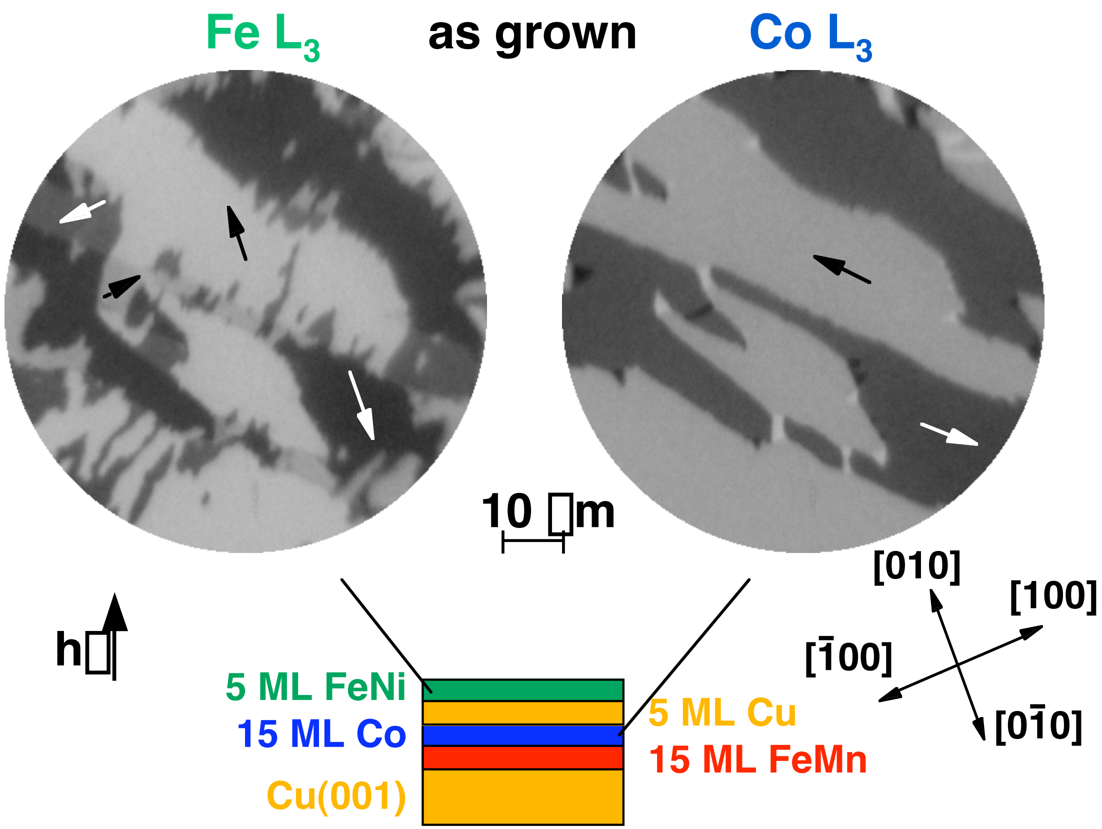

L. I. Chelaru, F. Offi, M. Kotsugi, and W. Kuch, MPI-MSP (unpublished)

XMCD-PEEM: layer-resolved magnetic imaging

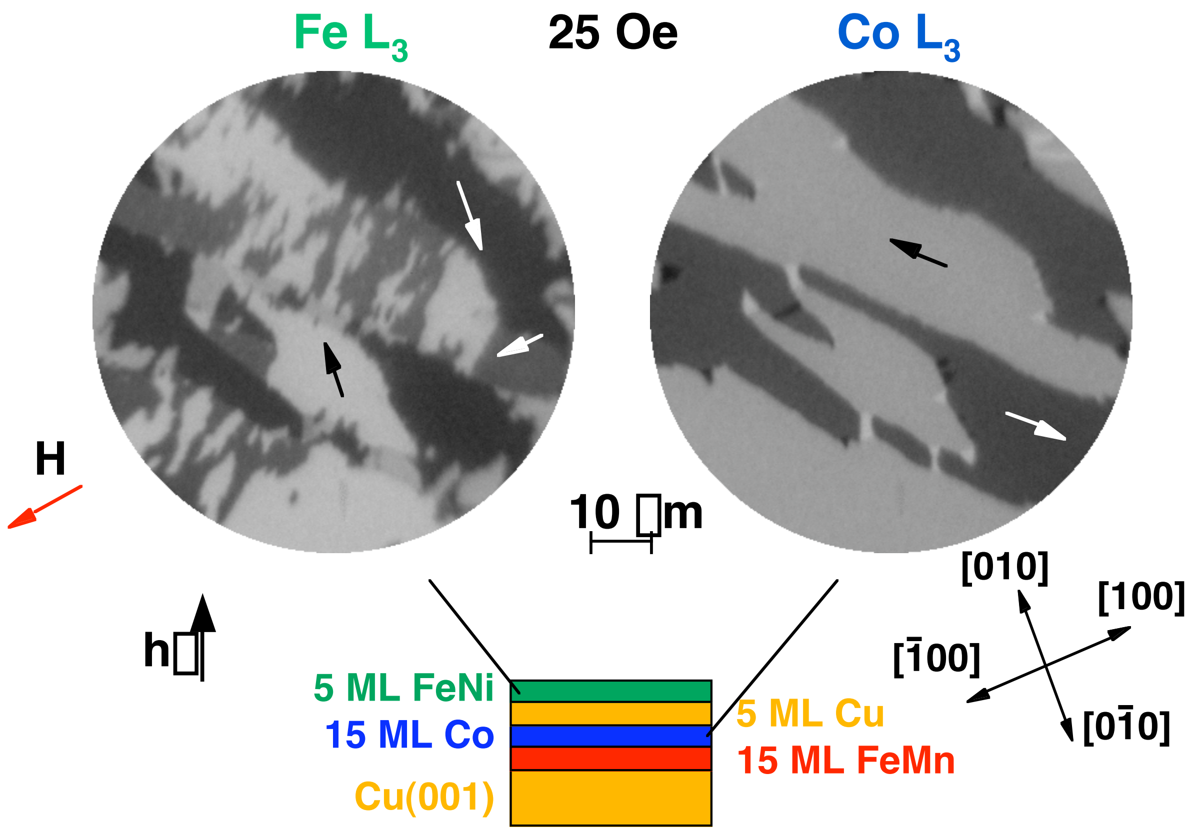

L. I. Chelaru, F. Offi, M. Kotsugi, and W. Kuch, MPI-MSP (unpublished)

XMCD-PEEM: layer-resolved magnetic imaging

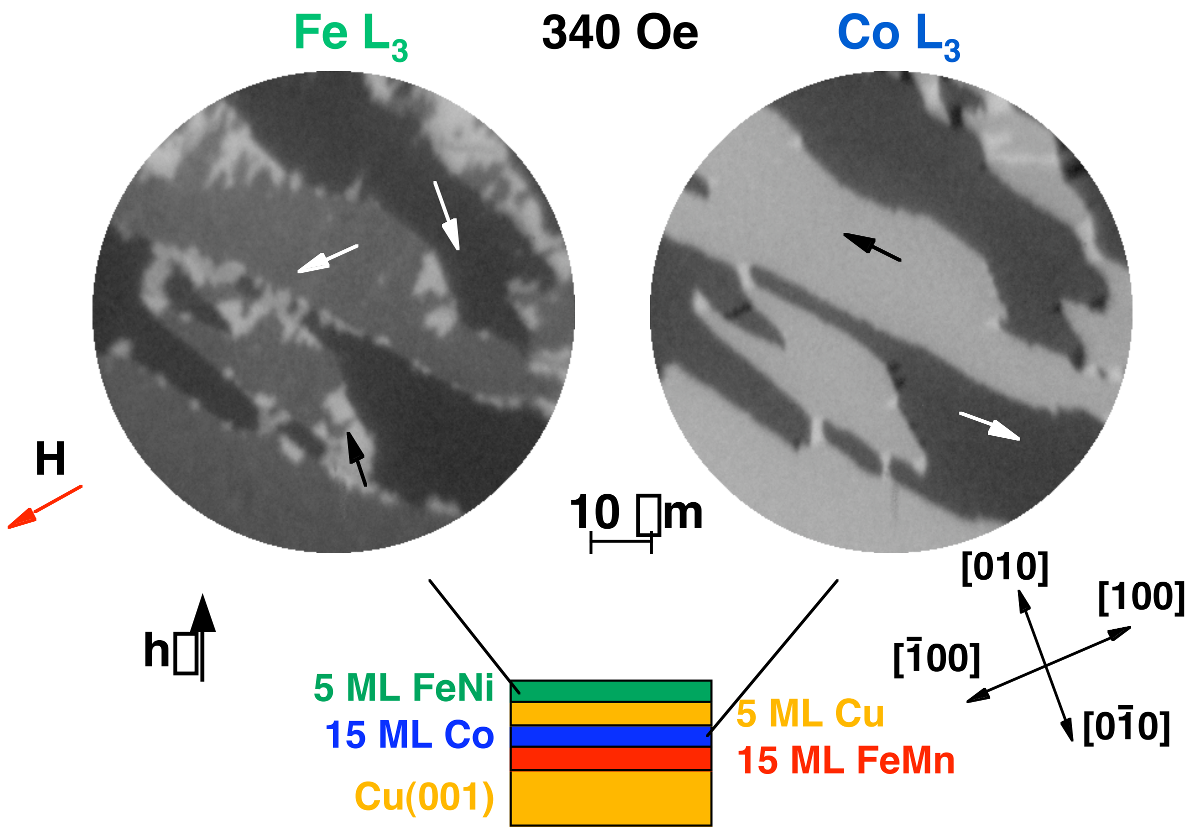

L. I. Chelaru, F. Offi, M. Kotsugi, and W. Kuch, MPI-MSP (unpublished)

XMCD-PEEM

- element specific, can be used for layer-specificity
- needs synchrotron radiation
- good resolution
- parallel imaging
- moderately surface sensitive (≈ 20...100 Å)
- sensitive to external magnetic fields
- in vacuum
- vectorial information by rotating sample
- quantitative spectroscopic information available (“sum-rule microscopy”)

spin-polarized low energy electron microscopy (SPLEEM)

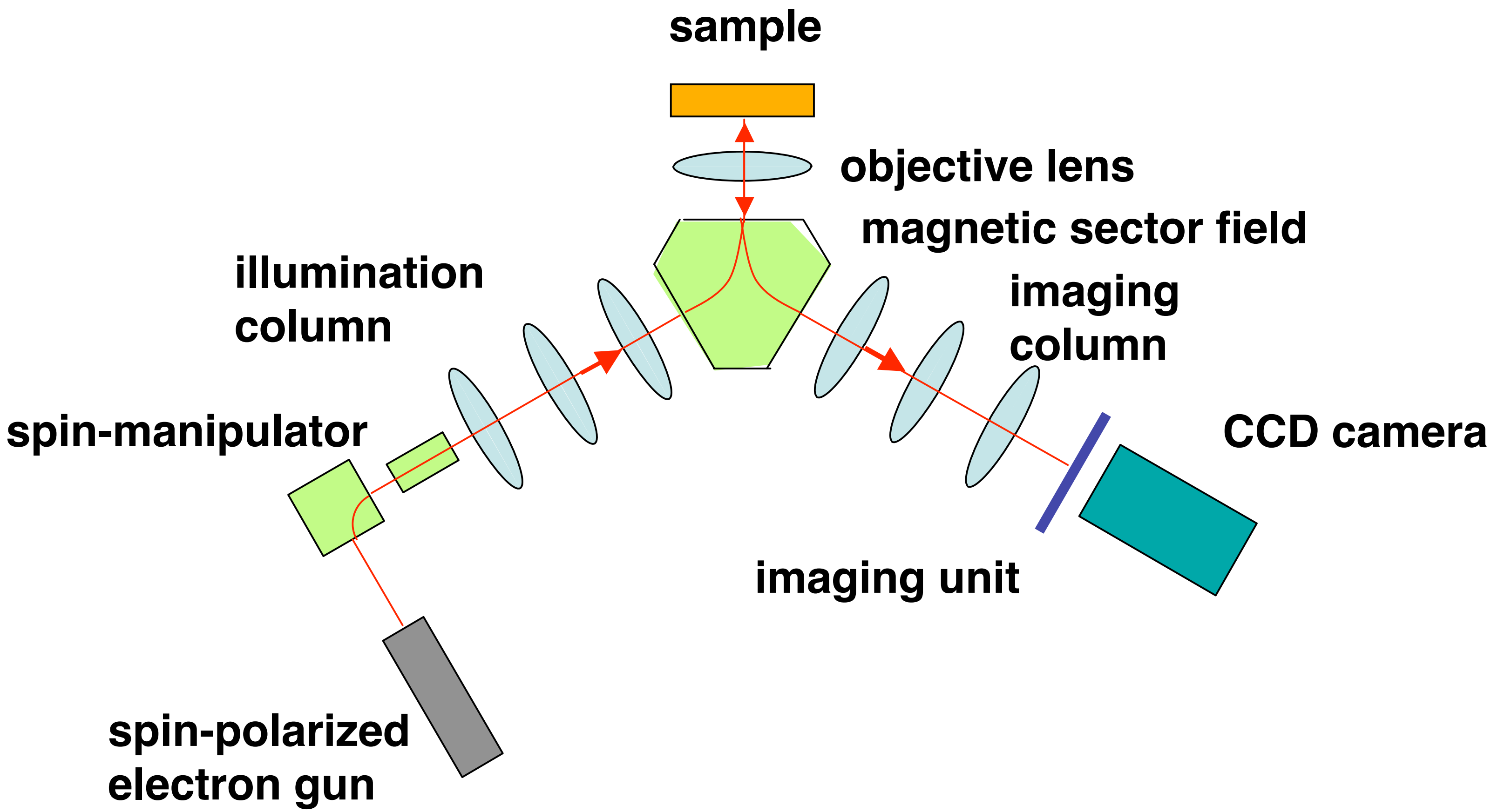

spin-polarized low energy electron microscopy (SPLEEM)

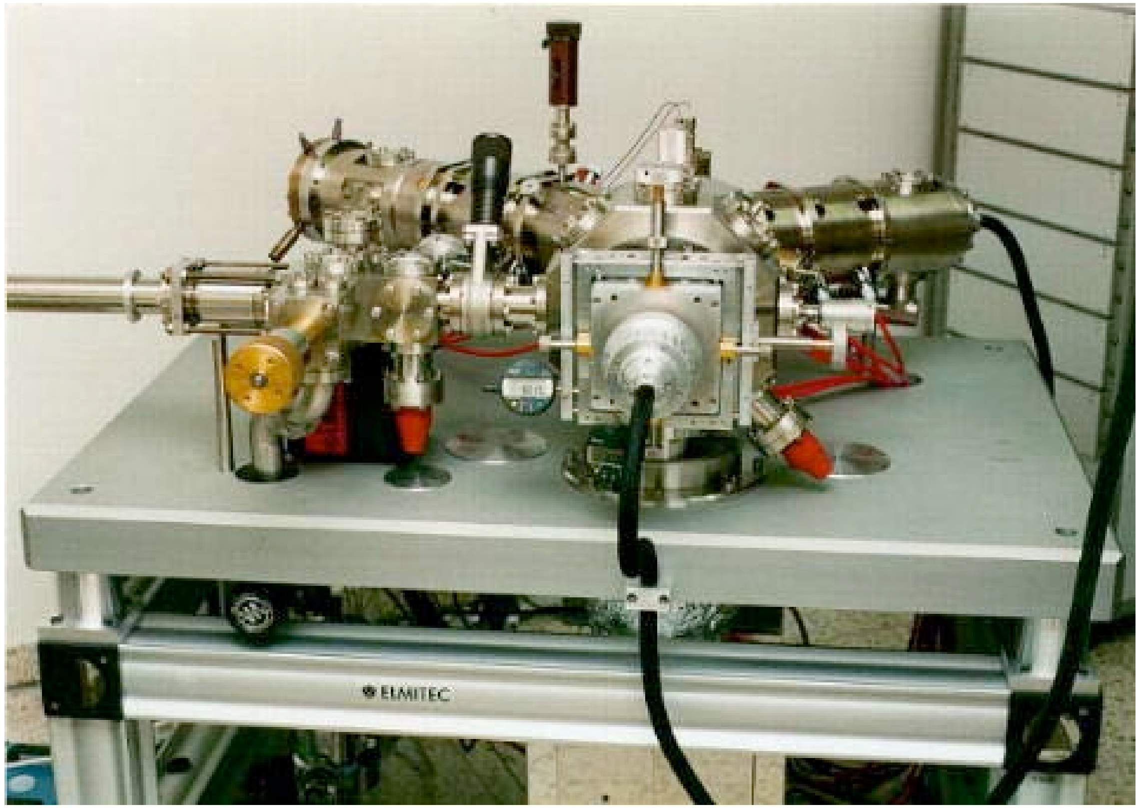

(Elmitec LEEM 3)

SPLEEM

spin manipulation

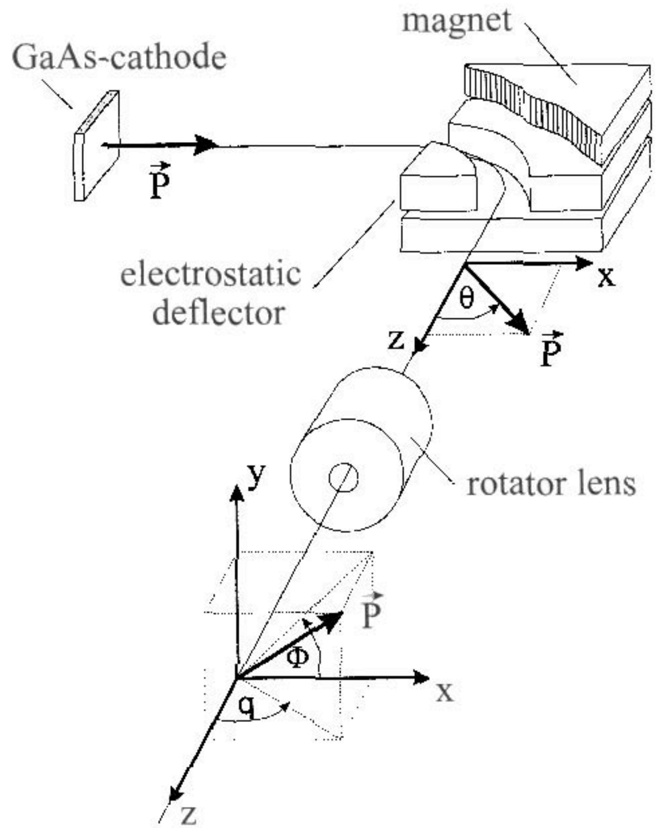

magnetic contrast

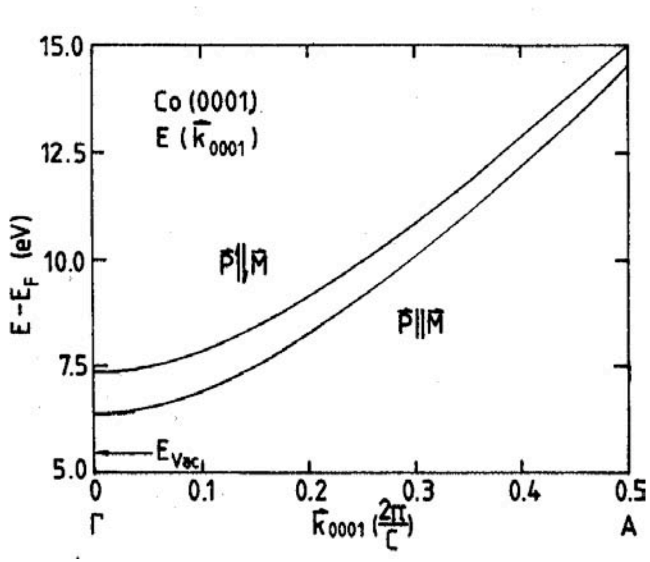

Th. Duden and E. Bauer, Surf. Rev. Lett. 5 (1998) 1213

SPLEEM: example

magnetization “wrinkle” in Co/W(110)

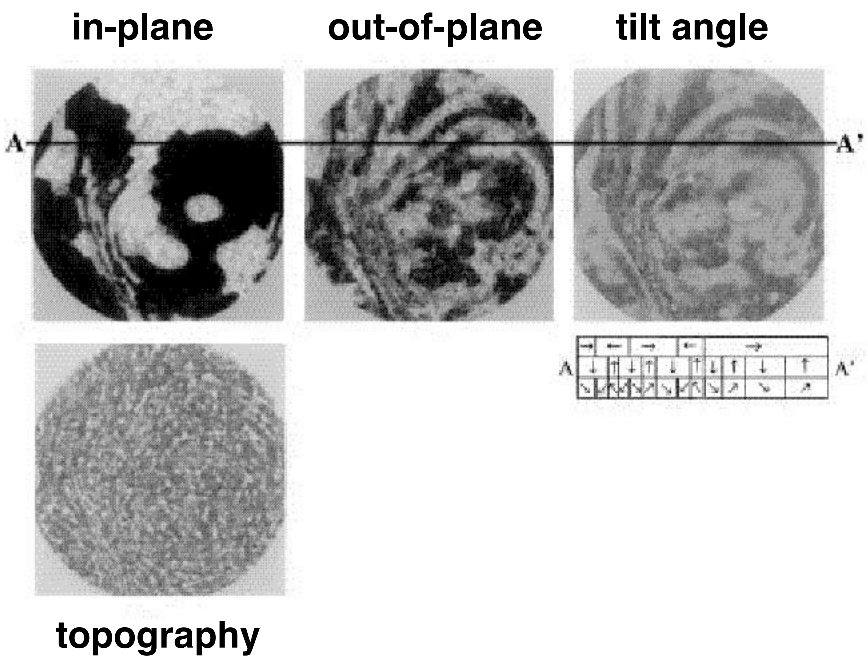

T. Duden and E. Bauer, PRL 77 (1996) 2308

SPLEEM: another example

during deposition of
Fe/Cu(001),
growth rate: 0.080 ML/min
E = 1.8 eV

2.13 ML
2.20 ML
2.33 ML
2.87 ML

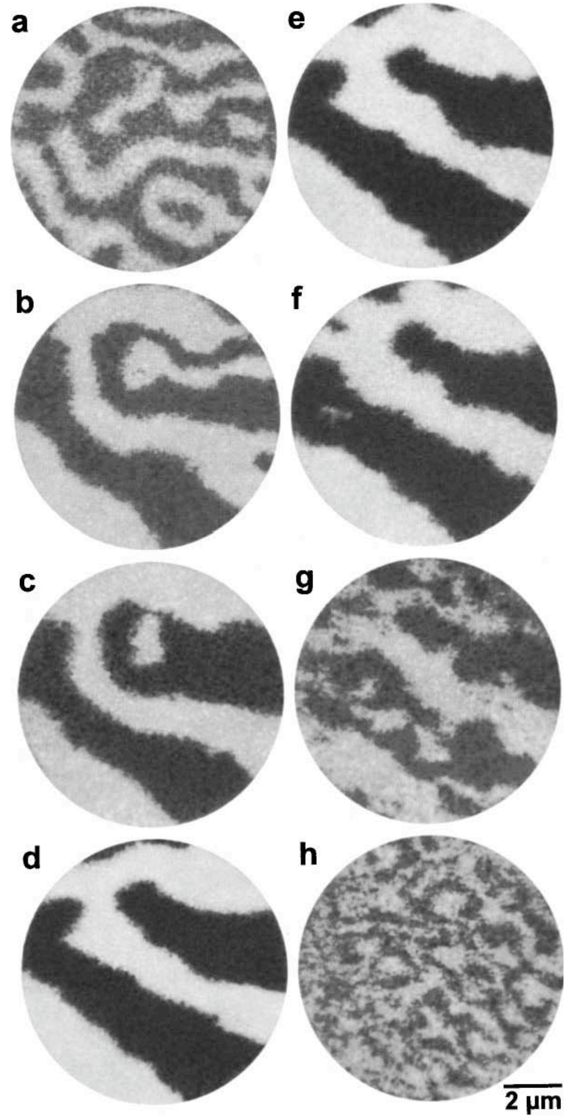

3.13 ML
3.29 ML
3.60 ML
3.83 ML

K. L. Man et al., PRB 65 (2001) 024409

Topographic LEEM contrast

atomic steps at the surface of Cu(001)

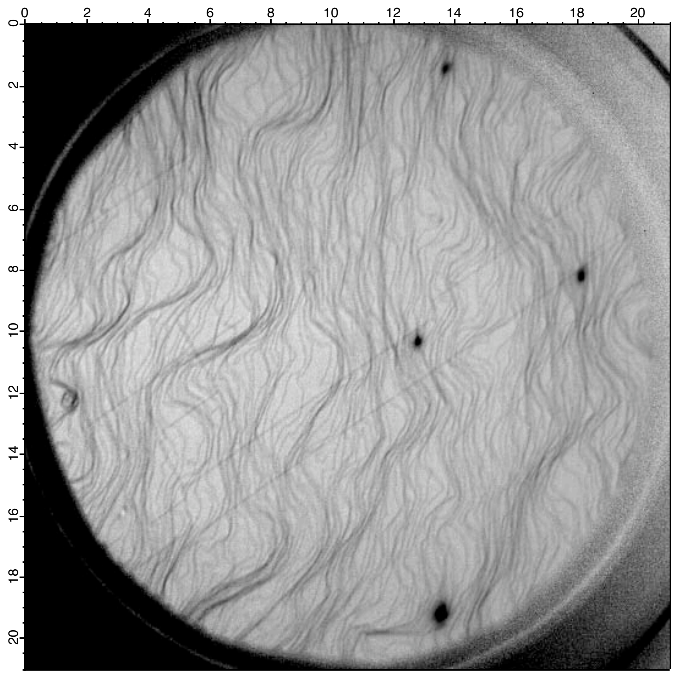

W. Kuch, K. Fukumoto, J. Wang, MPI-MSP,
C. Quitmann, F. Nolting, T. Ramsvik, PSI-SLS, unpublished.

SPLEEM

- surface sensitive
- fast
- vectorial measurement without turning sample
- small field of view possible due to electron beam focusing
- topographic information simultaneously available
- conditions for best contrast depend on sample
- sensitive to external magnetic fields
- needs UHV
- not element specific

Zone plate as x-ray lens

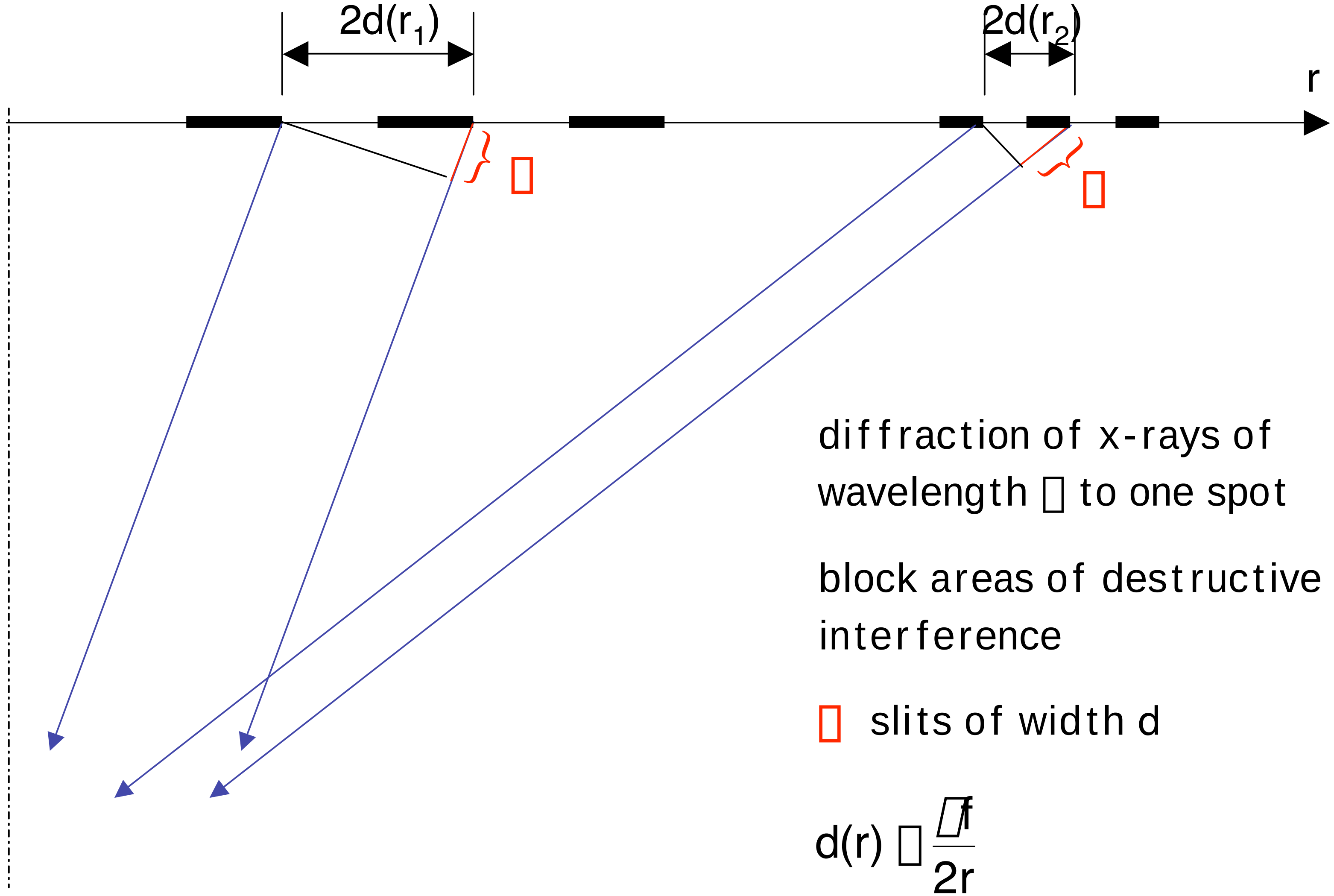

diffraction of x-rays of wavelength λ to one spot

block areas of destructive interference

⇒ slits of width d

$$d(r) \approx \frac{\lambda f}{2r}$$

Zone plate as x-ray lens

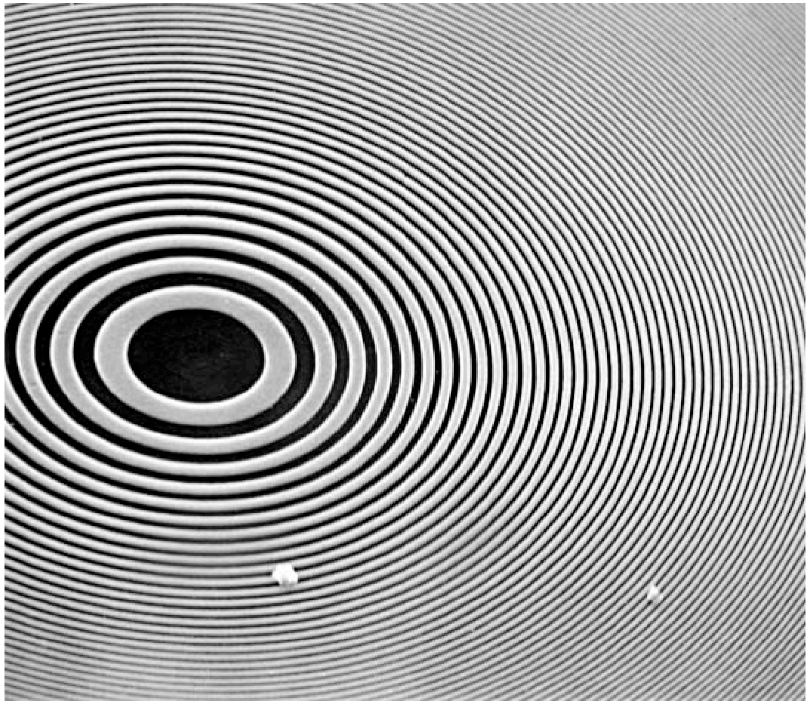

inner part of a zone plate lens.
diameter: 45 µm,
outermost zone: 35 nm wide.

from: homepage of Center for X-ray Optics,
Lawrence Berkeley National Laboratory

Transmission x-ray microscopy (TXM)

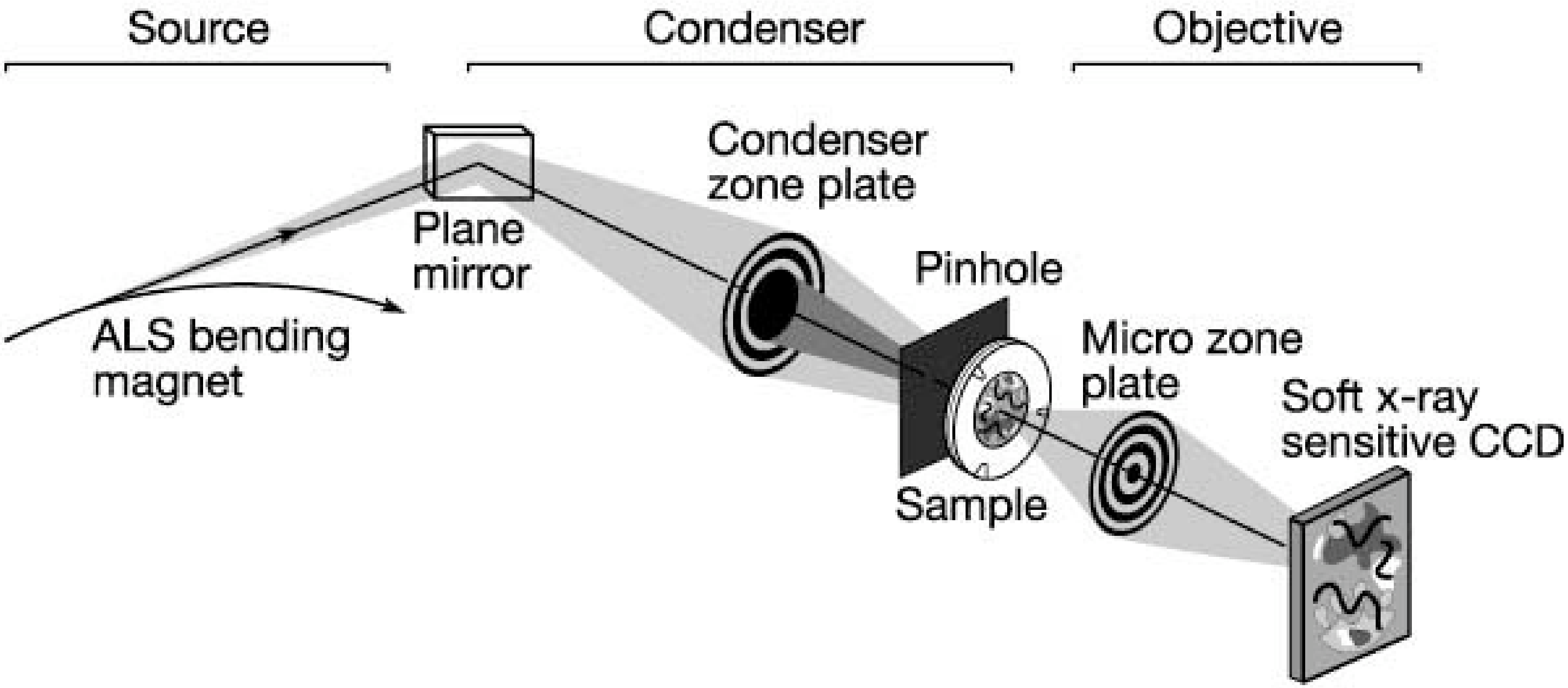

G. Denbeaux et al., IEEE Trans. Mag. 37 (2001) 2764

M-TXM: example

magneto-optical storage media

50 nm $Tb_{25}Fe_{56}Co_{19}$

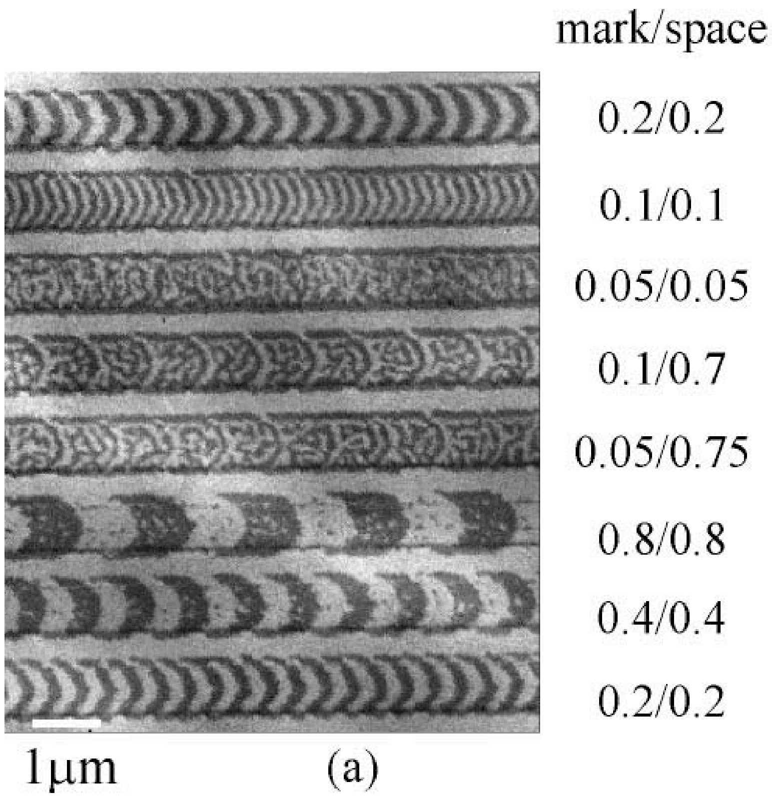

P. Fischer et al., Rev. Sci. Instrum. 72 (2001) 2322

M-TXM: example

[Fe/Gd] nanostripes

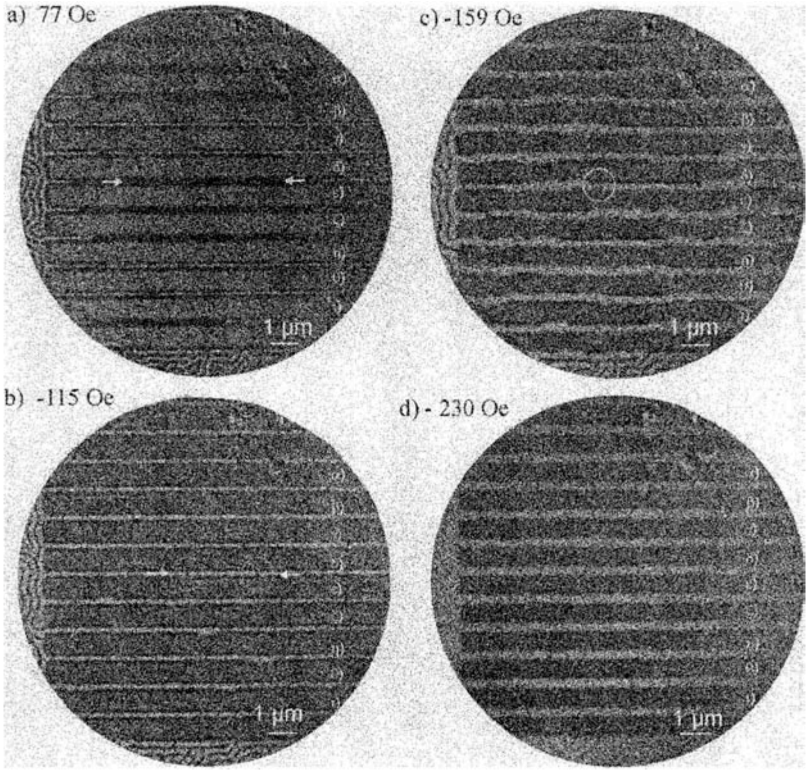

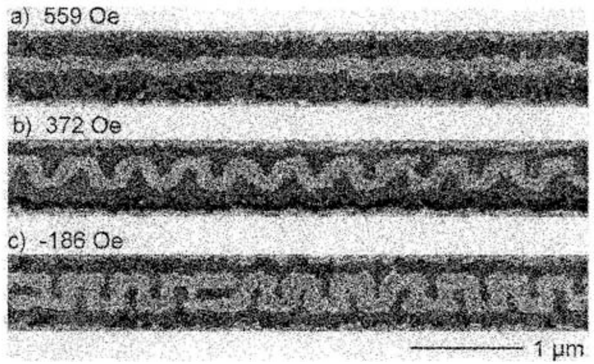

T. Eimüller et al., J. Phys. IV 104 (2003) 483

New high-resolution zone plate

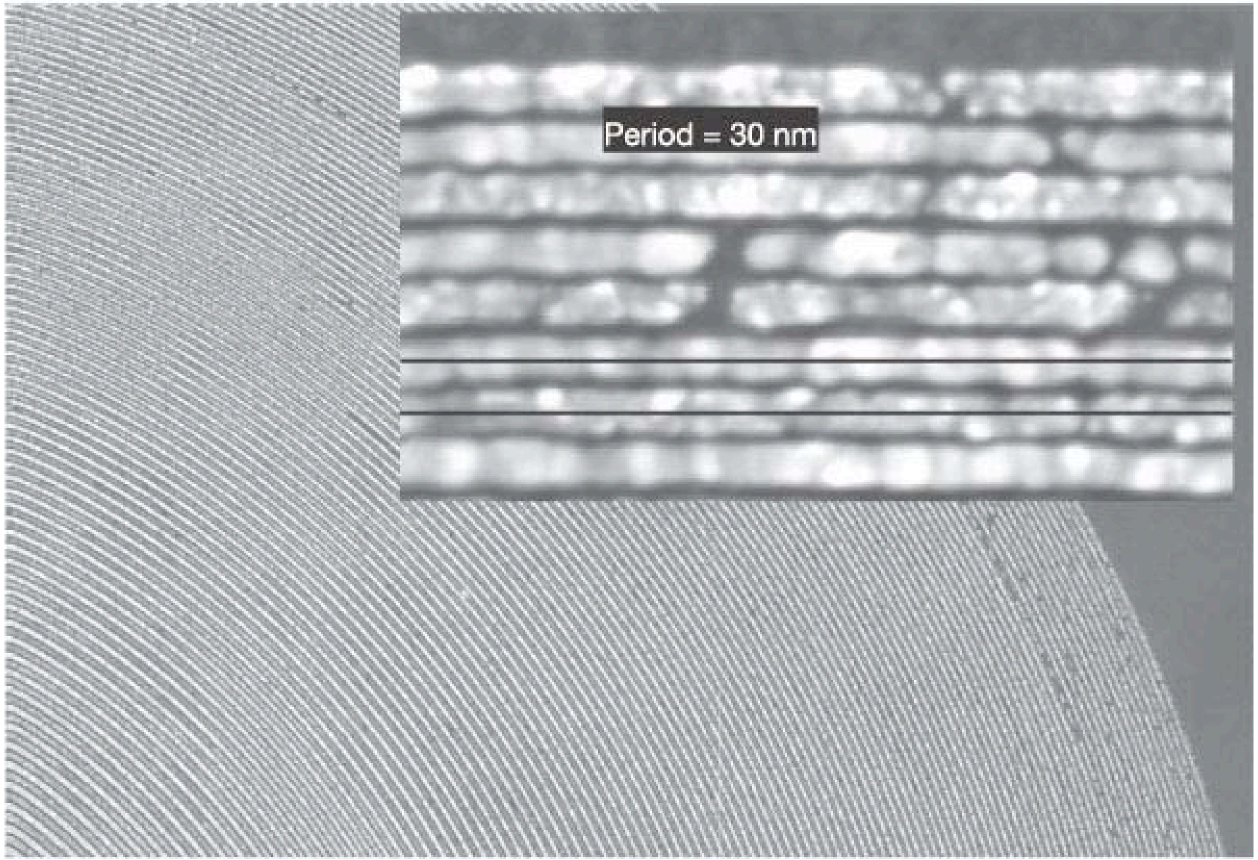

W. Chao et al., Nature 435, 1210 (2005)

New high-resolution zone plate

images of test object with 19.5 nm lines and spaces

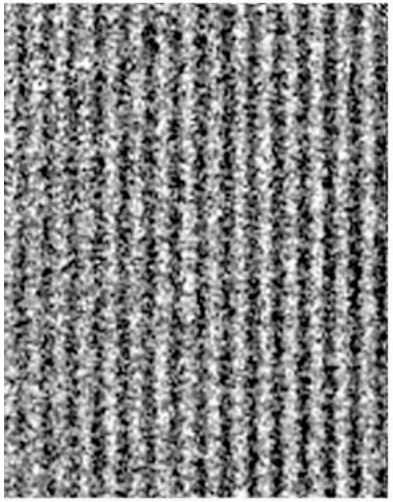

25-nm zoneplate

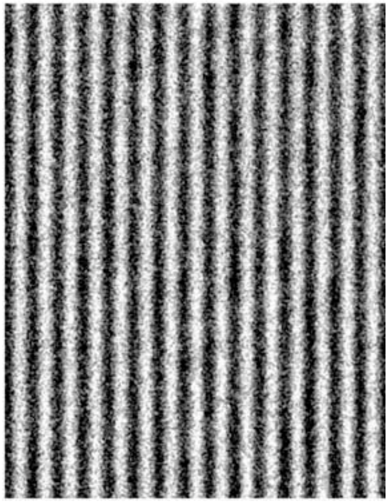

15-nm zoneplate

images of test object with 15.1 nm lines and spaces

25-nm zoneplate

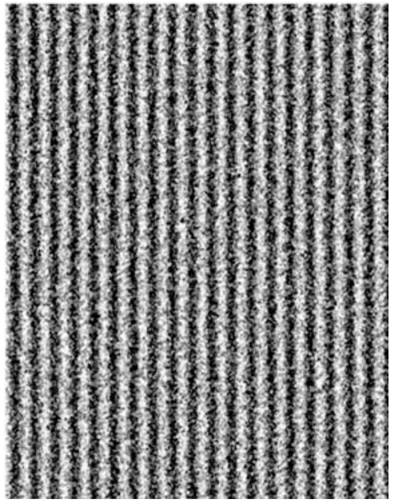

15-nm zoneplate

W. Chao et al., Nature 435, 1210 (2005)

M-TXM

- high resolution
- element specific, can be used for layer-specificity
- needs synchrotron radiation
- insensitive to magnetic fields
- parallel imaging or scanning
- only in transmission
- does not need UHV

When samples start looking at you...

LEEM image of steps on Si(100), FOV: 4 µm

G. L. Kellogg, Sandia Natl. Lab., Albuquerque

...it's time for a break!

Linear magnetic dichroism in soft x-ray absorption (XMLD)

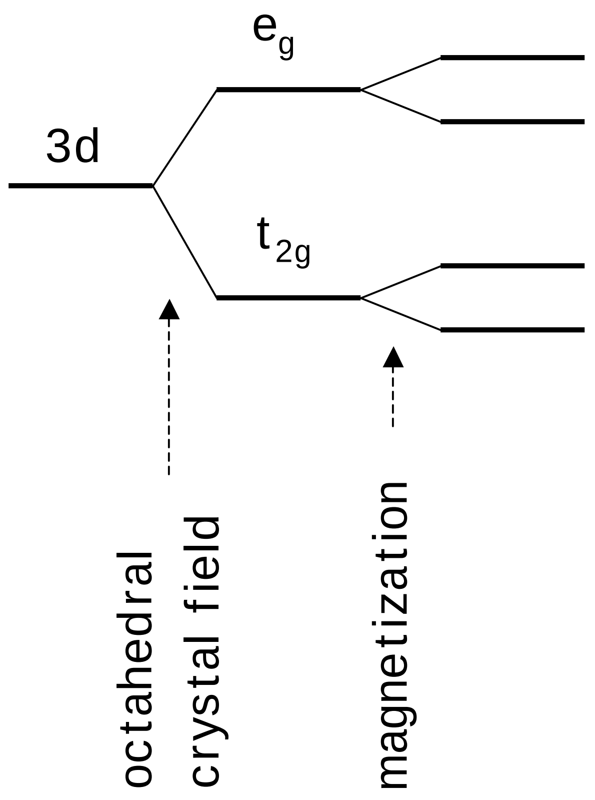

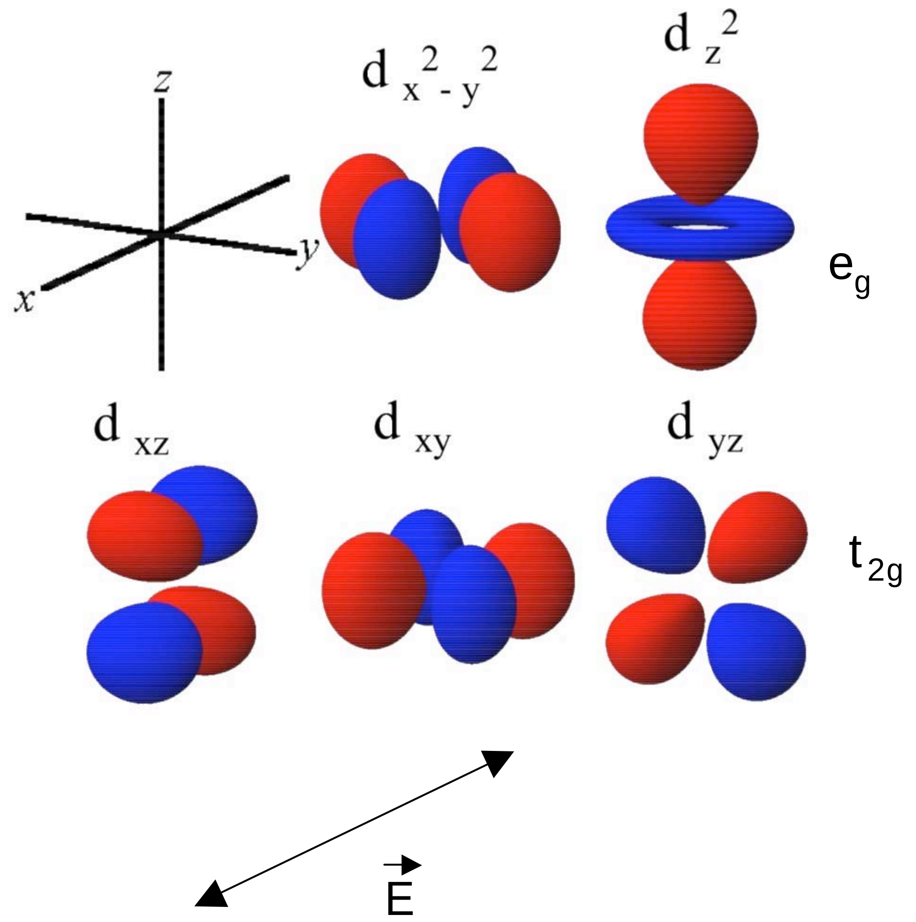

Linear magnetic dichroism in soft x-ray absorption (XMLD)

<u>oxide</u>

NiO/MgO(001)

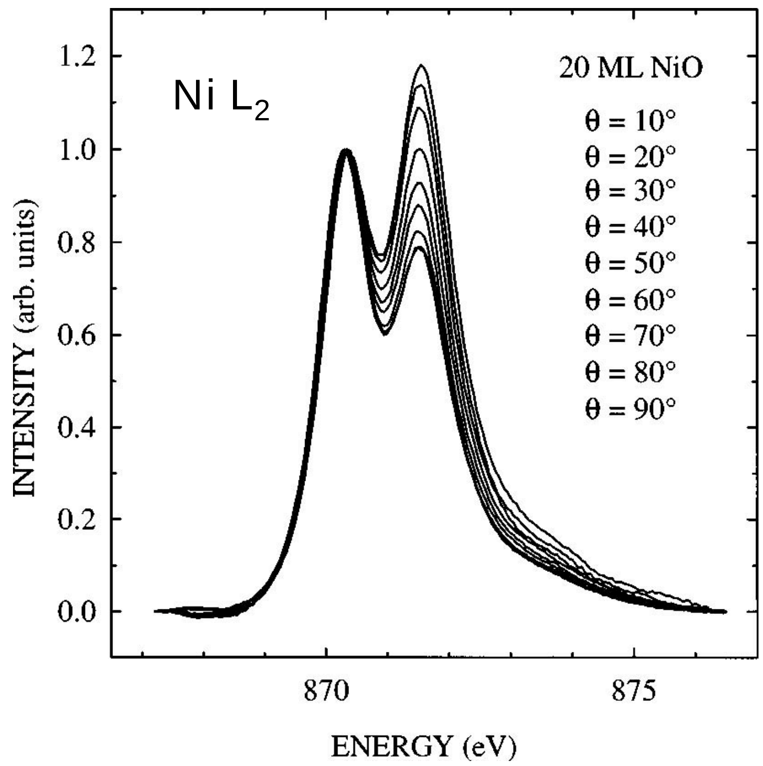

D. Alders et al., Phys. Rev. B 57 (1998) 11623

<u>metal</u>

Co/Cu(001)

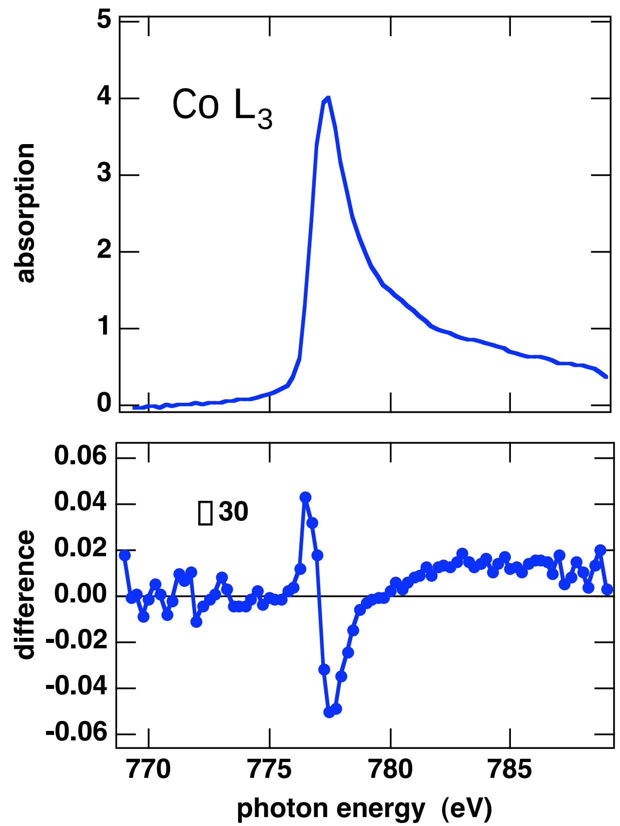

W. Kuch et al.,
Phys. Rev. Lett. 92 (2004) 017201

XMLD as contrast mechanism in PEEM

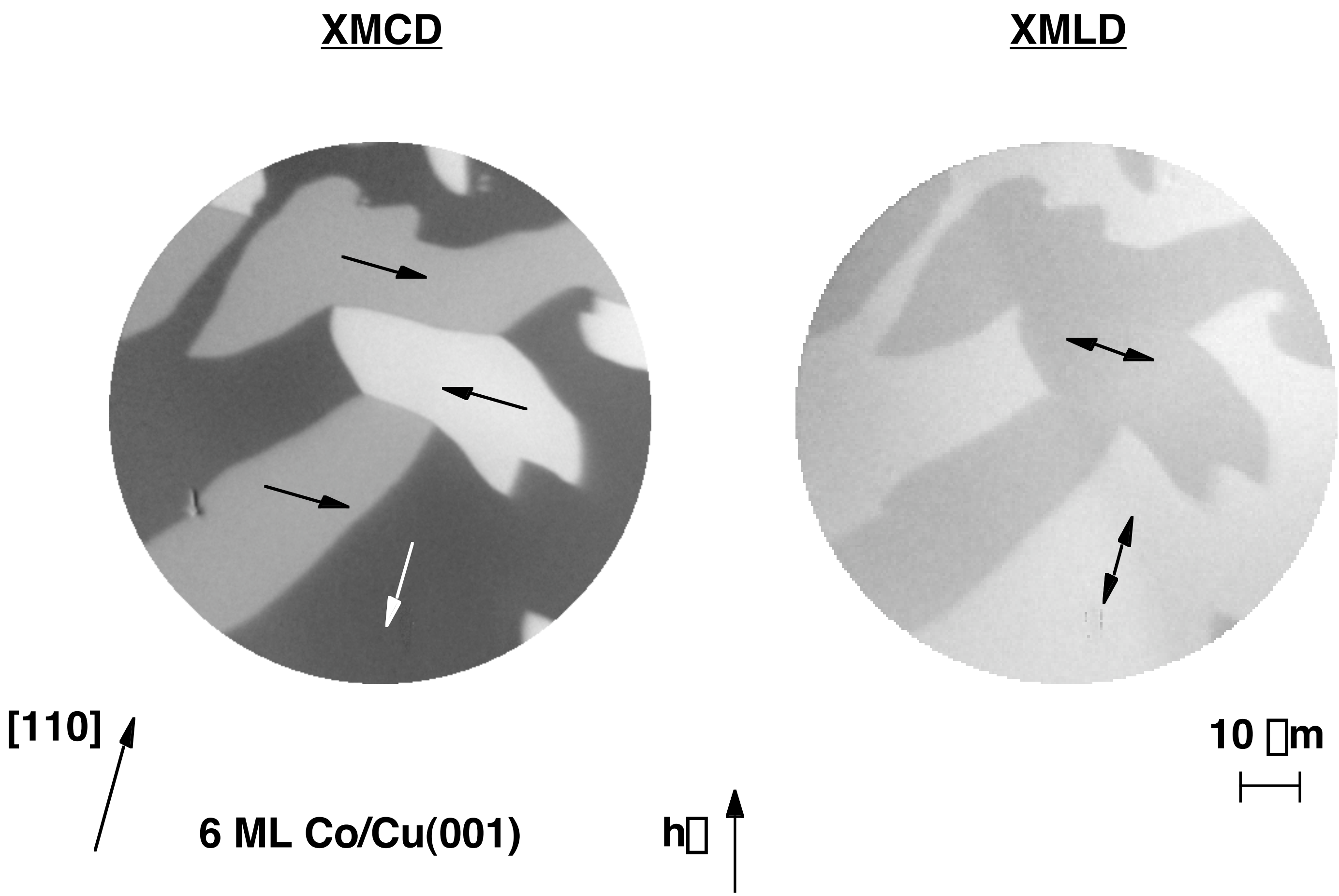

W. Kuch, F. Offi, L. I. Chelaru, M. Kotsugi, J. Wang, and K. Fukumoto,
MPI-MSP (unpublished)

XMLD as contrast mechanism in PEEM

Ni XMLD Co XMCD

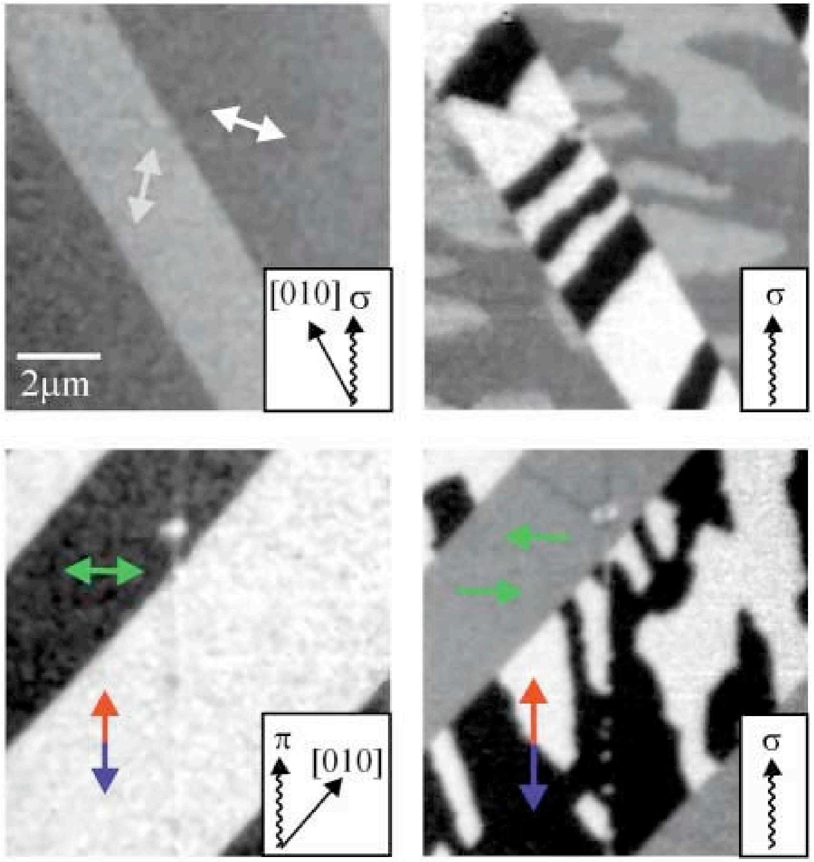

8 ML Co/NiO(001)

H. Ohldag et al., Phys. Rev. Lett. 86 (2001) 2878

Imaging electron energy analyzers

highpass filter

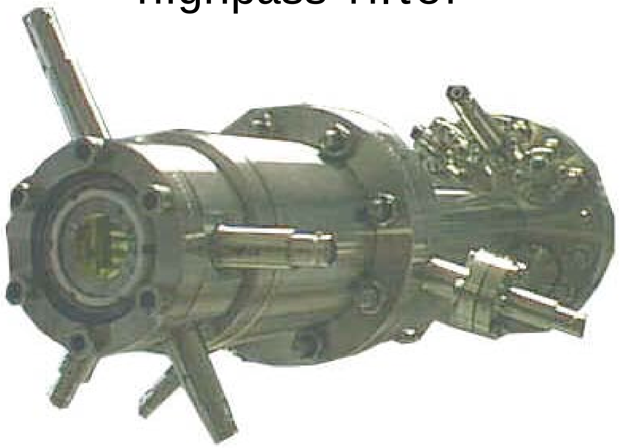

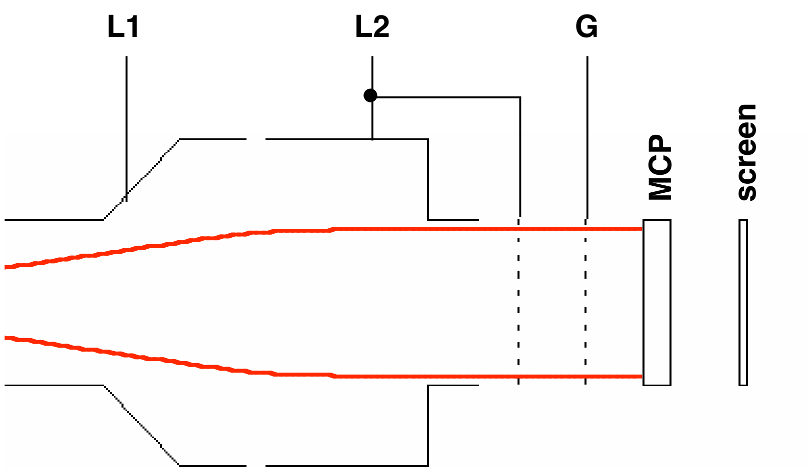

retarding field analyzer

e^- with $E_{kin} > e \cdot U_G$ can pass grid G (highpass)

bandpass filter

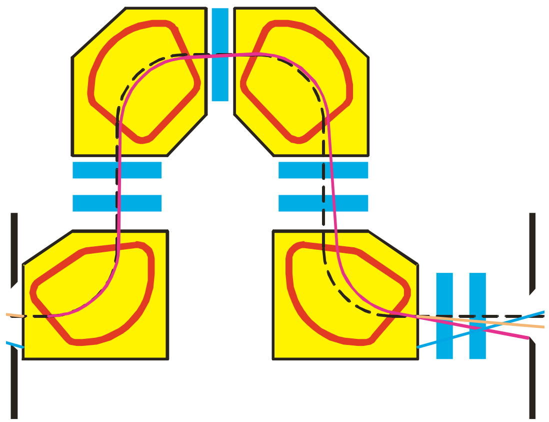

Photon absorption vs. electron emission spectroscopy

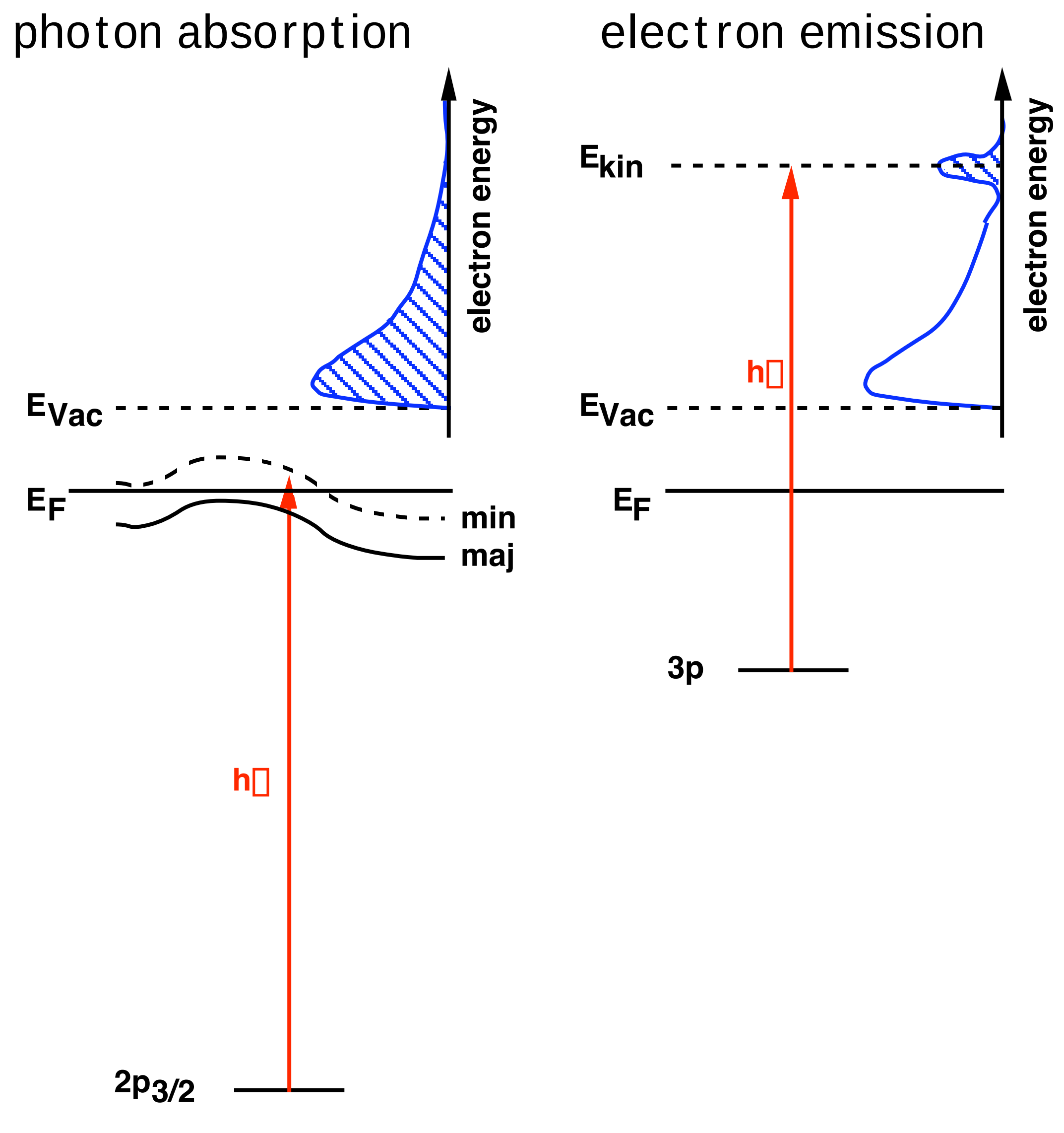

Magnetic linear dichroism in photoemission (MLDAD)

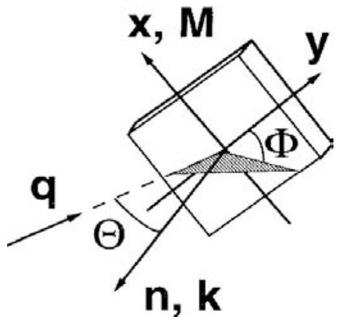

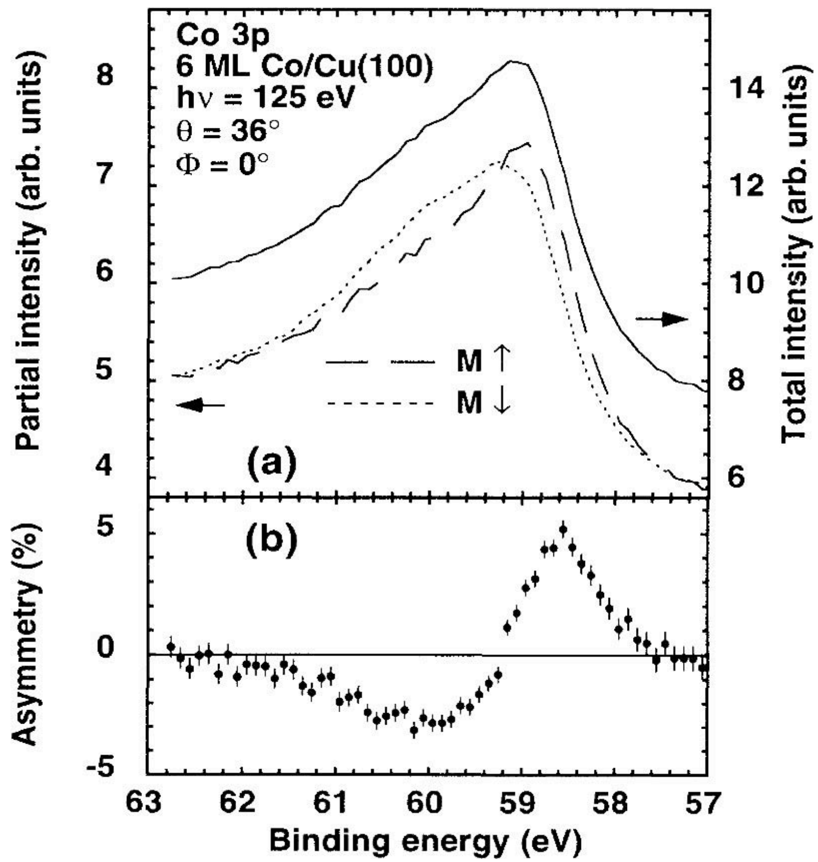

W. Kuch et al., Phys. Rev. B 51 (1995) 609

PEEM: absorption vs. photoemission

sensitivity:

Fe(001)

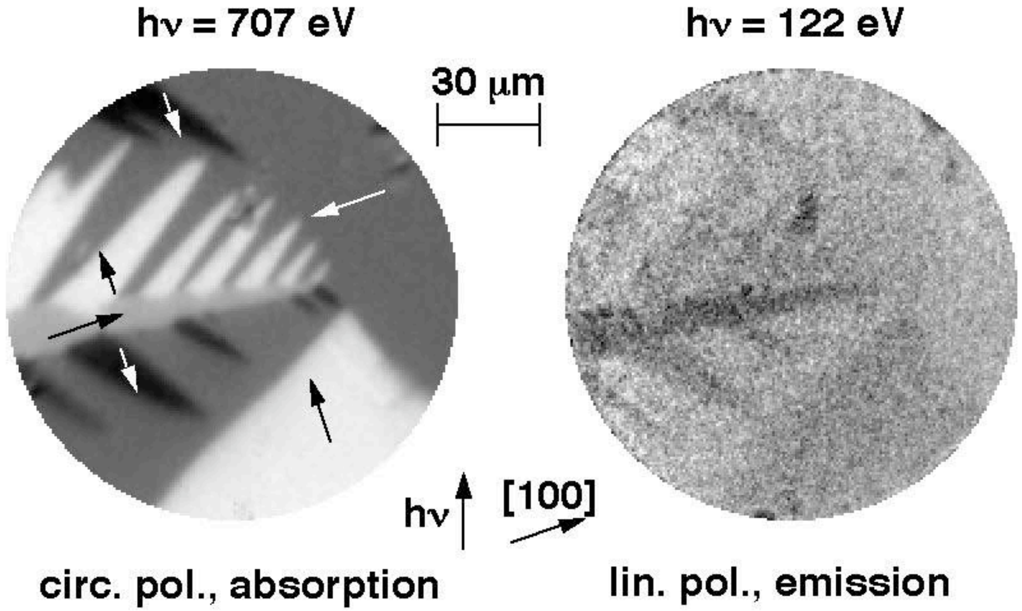

XMCD
absorption

MLDAD
photoemission

W. Kuch et al., unpublished
(see also: W. Kuch et al., J. Vac. Sci. Technol. B 20 (2002) 2543)

PEEM: imaging of the diffraction plane

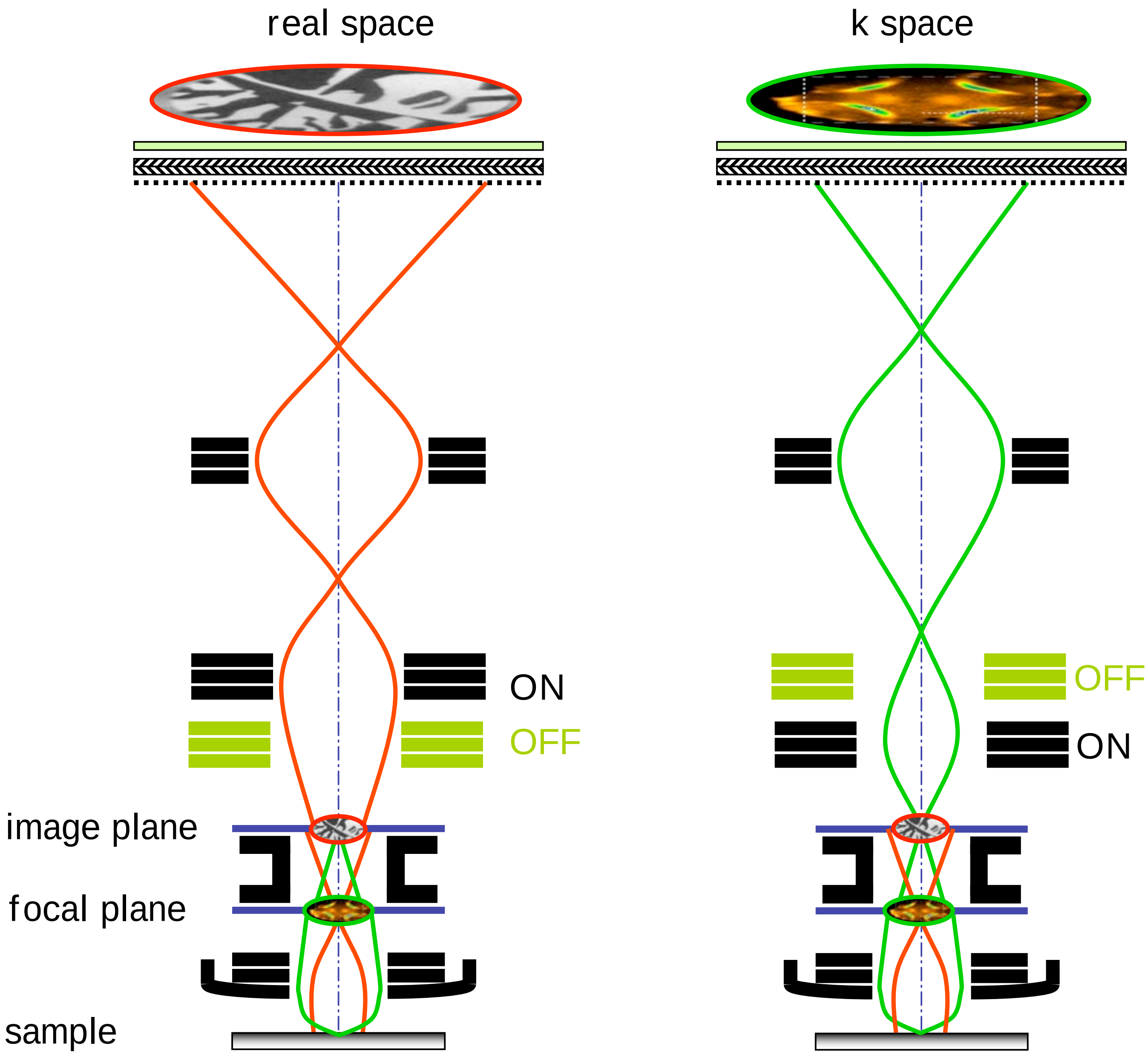

Fermi surface mapping by PEEM

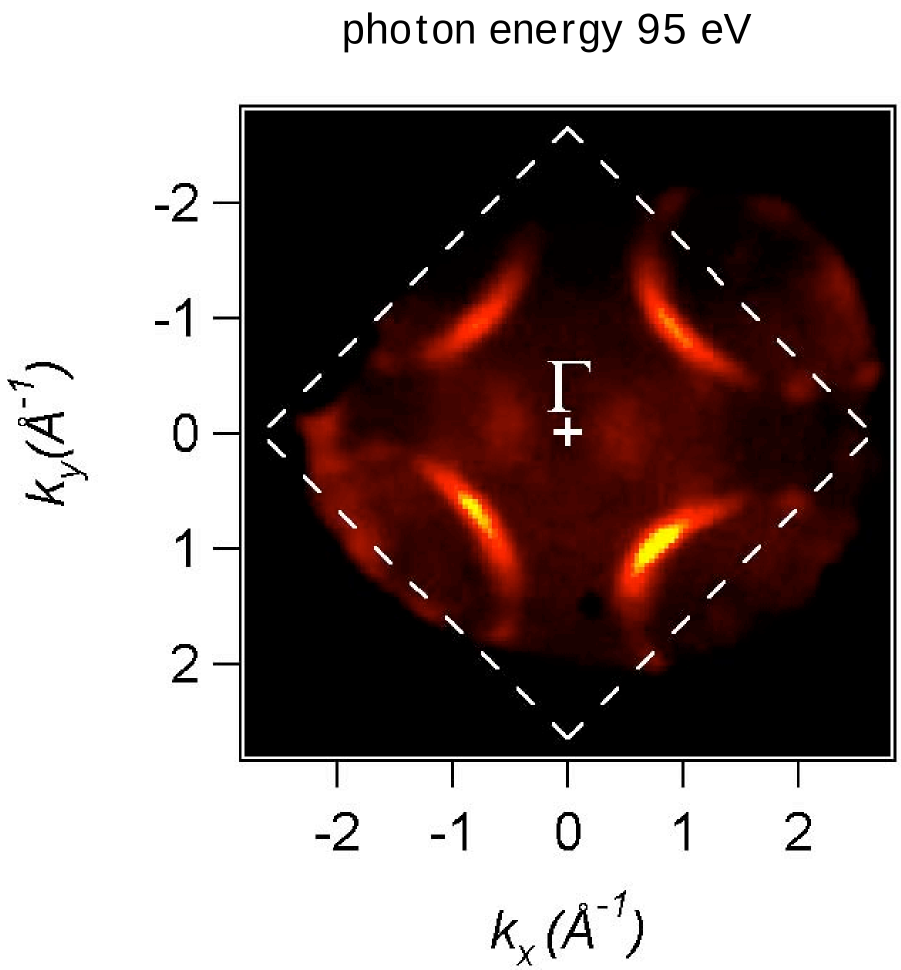

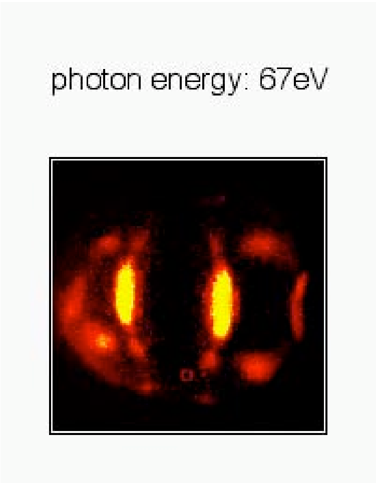

M. Kotsugi et al., Rev. Sci. Instrum. 74 (2003) 2754

Timescales in magnetic materials

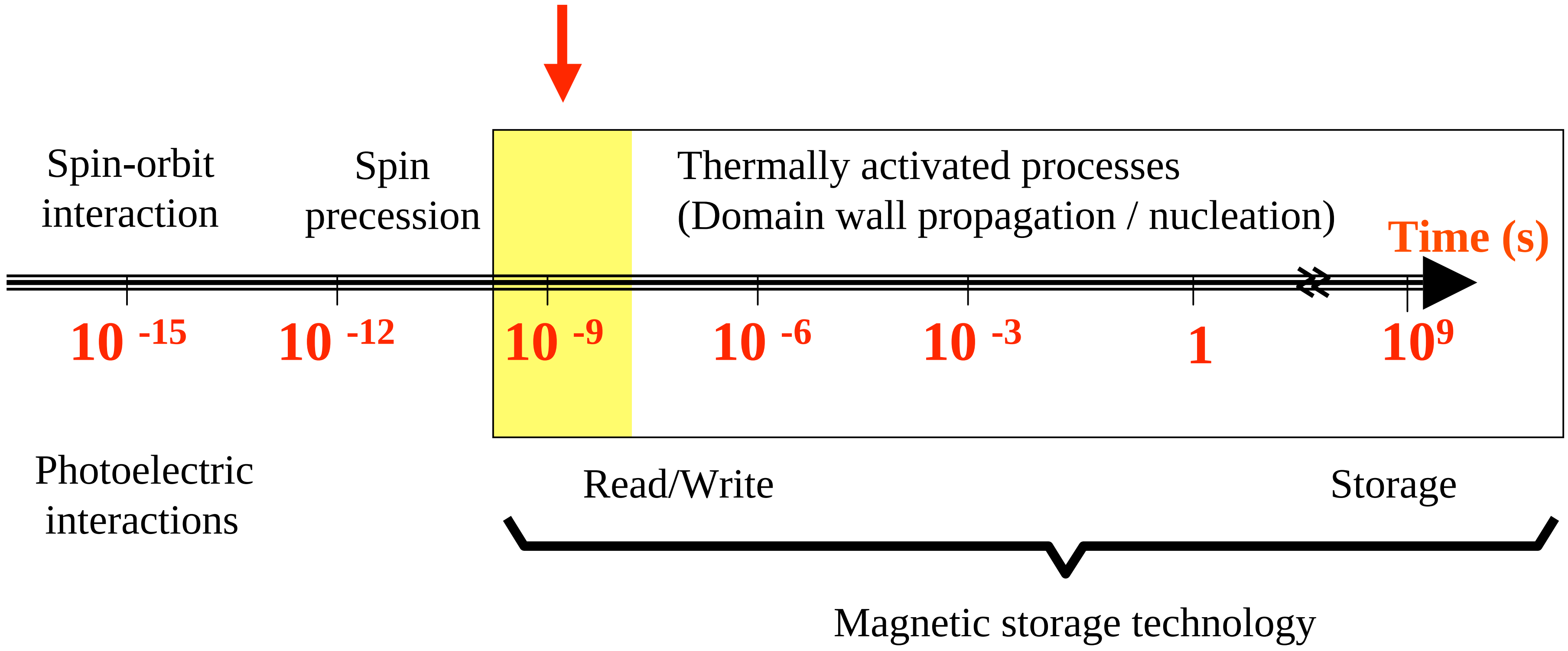

Time-resolved PEEM

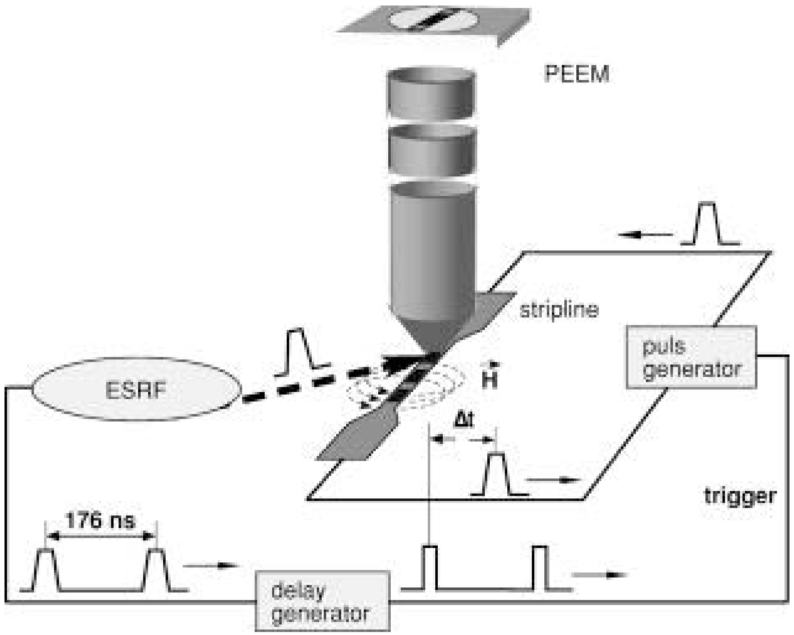

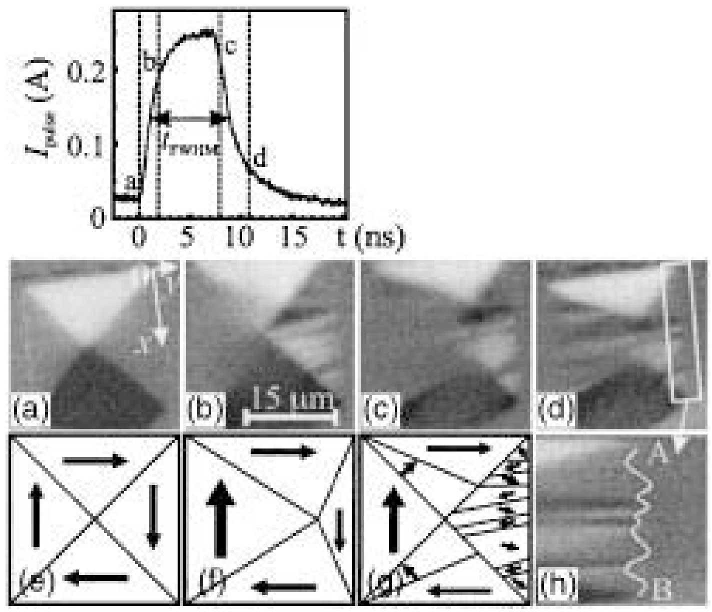

A. Kuksov et al.,
J. Appl. Phys. 95 (2004) 6530

C. M. Schneider et al.,
Appl. Phys. Lett. 85 (2004) 2562

Time-resolved PEEM

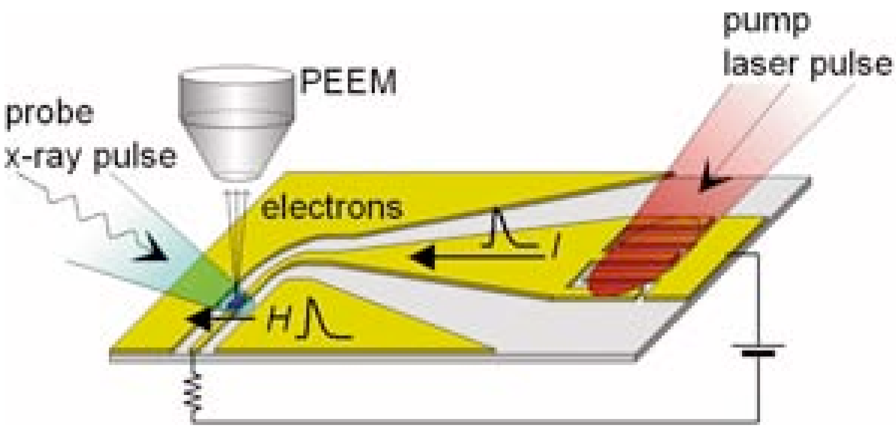

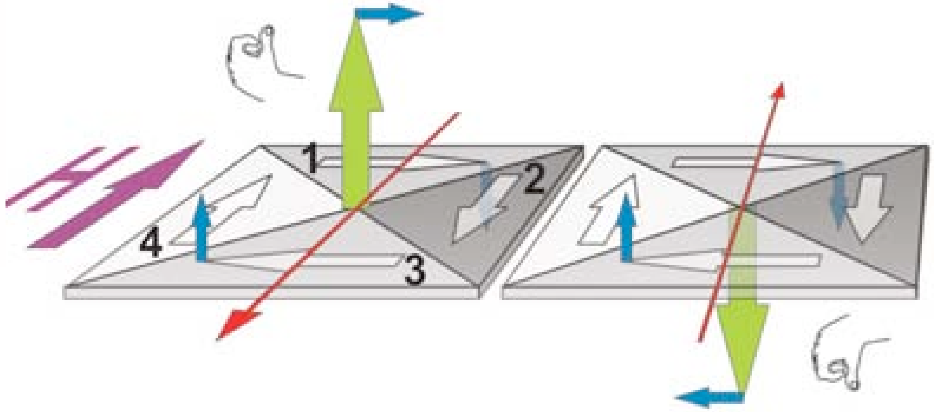

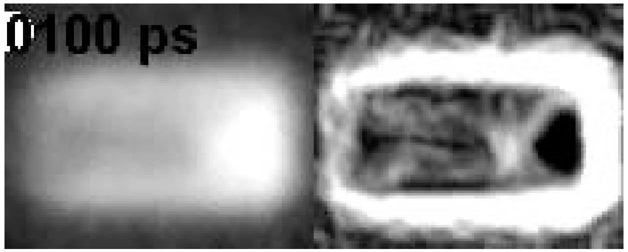

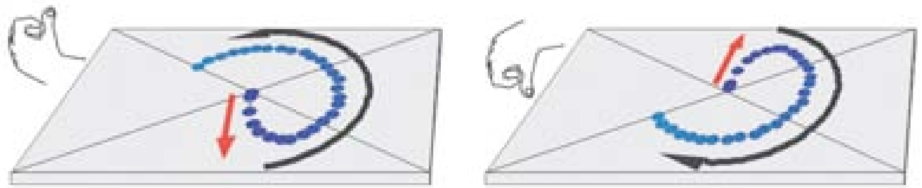

S.-B. Choe et al., Science 304 (2004) 420

Time-resolved M-TXM

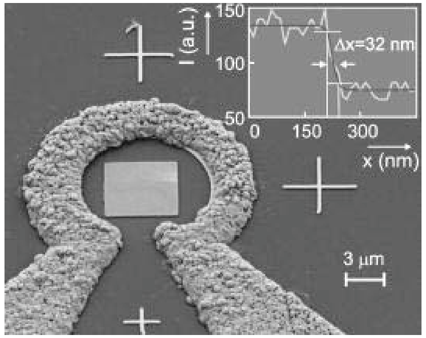

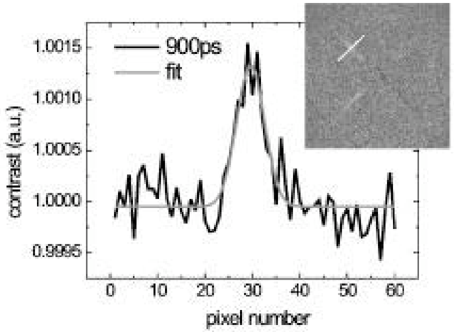

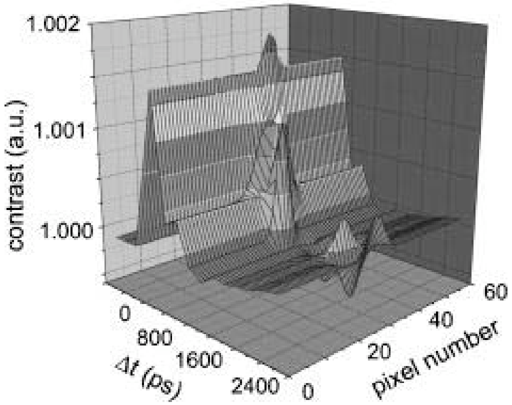

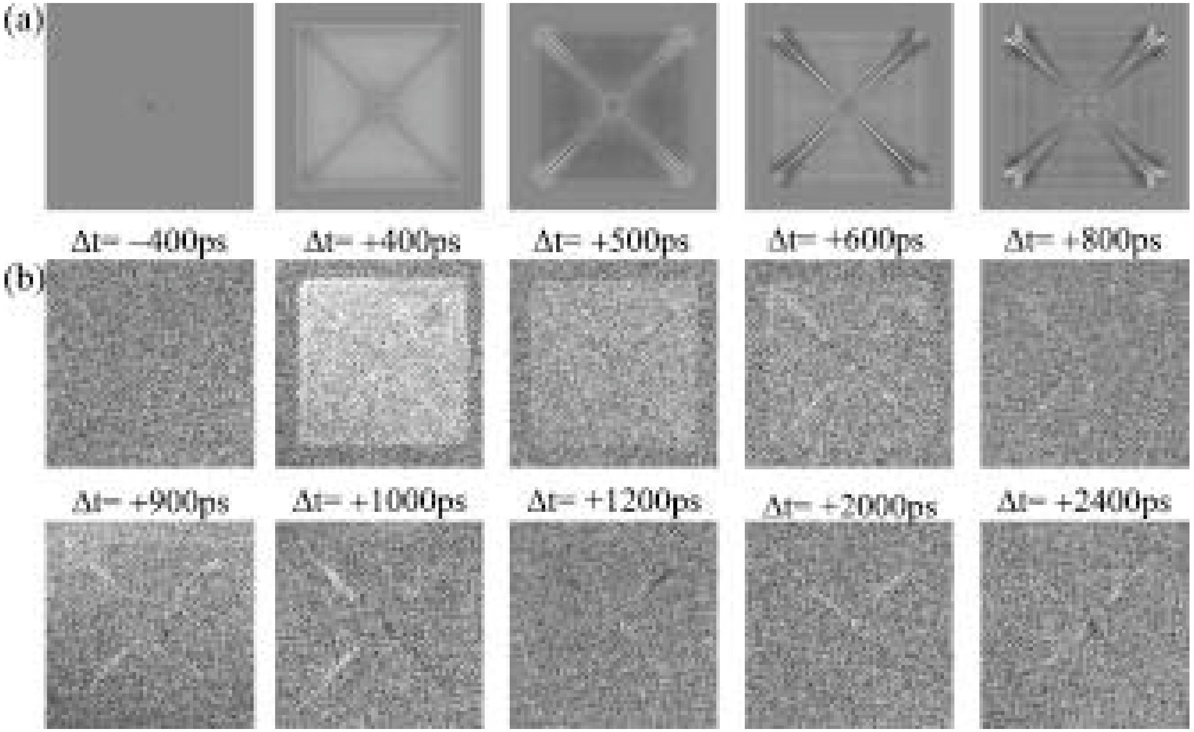

H. Stoll et al., Appl. Phys. Lett. 84 (2004) 3328

Time and layer resolved PEEM imaging

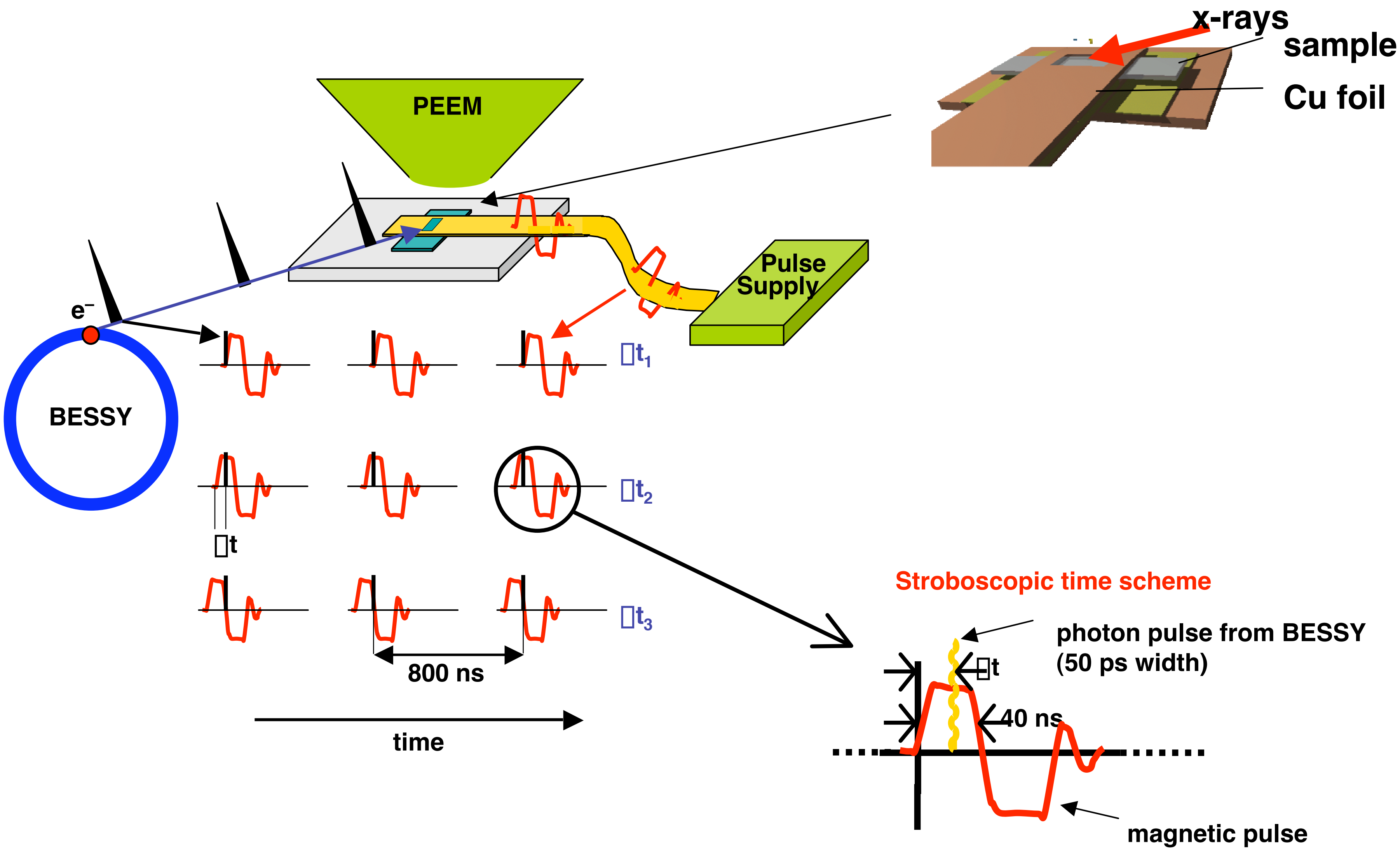

J. Vogel et al., Appl. Phys. Lett. 82 (2003) 2299

Time and layer-resolved PEEM imaging

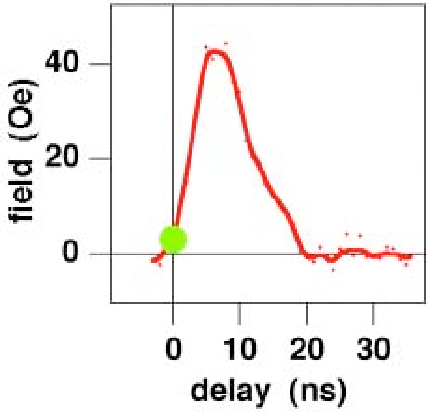

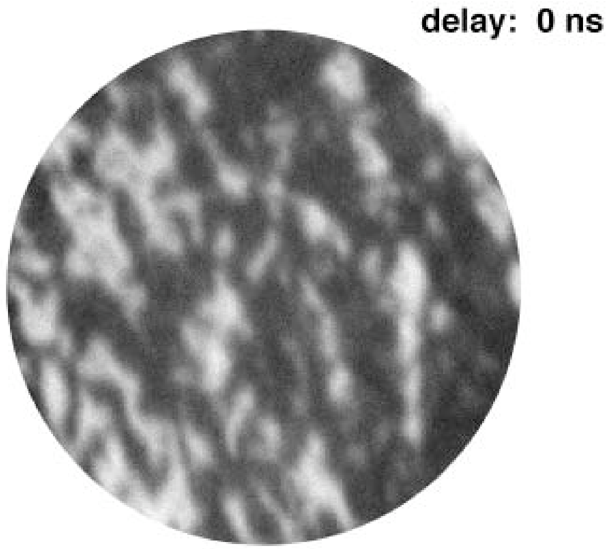

5 nm $Fe_{19}Ni_{81}$
4 nm Cu
5 nm Co

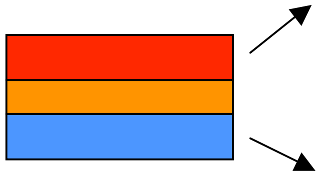

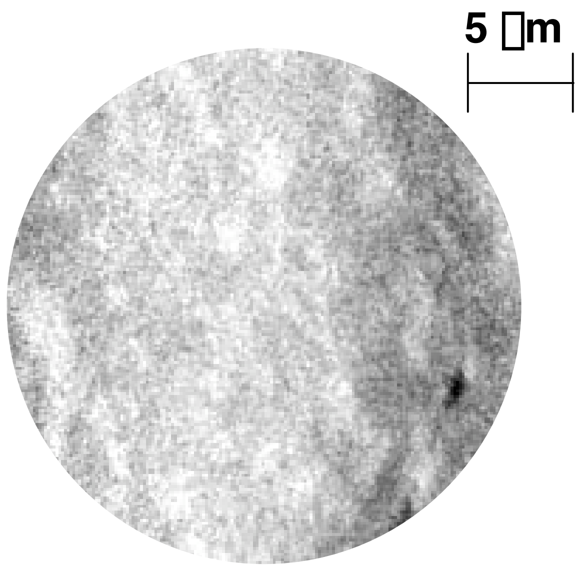

⇒ importance of domain wall energy for local domain wall speed

W. Kuch et al., Appl. Phys. Lett. 85 (2004) 440

Starting configuration

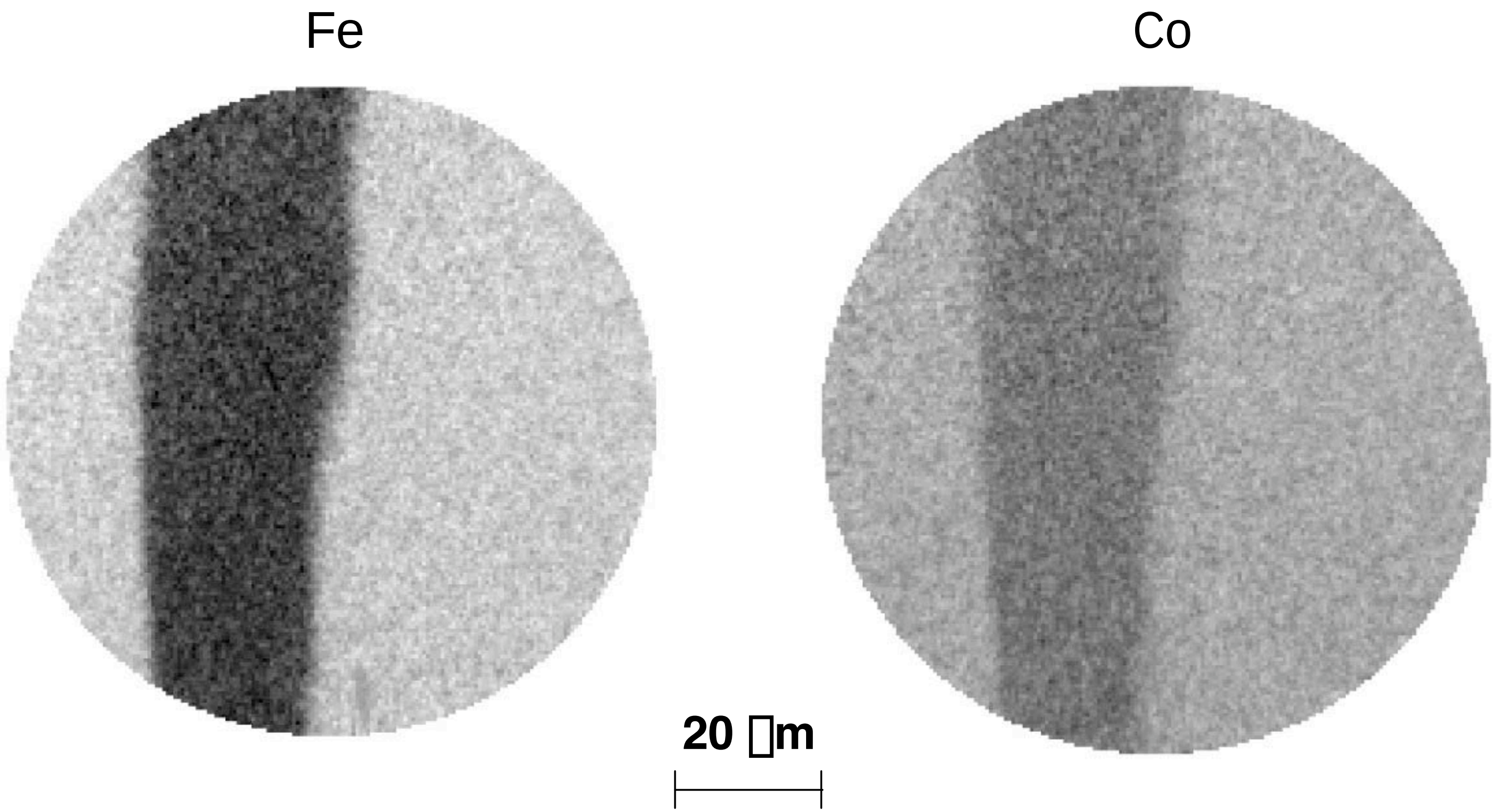

tunnel junction

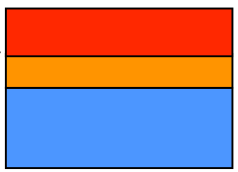

4 nm $Fe_{19}Ni_{81}$
2.5 nm Al_2O_3
7 nm Co

Layer-resolved stroboscopic magnetic microscopy

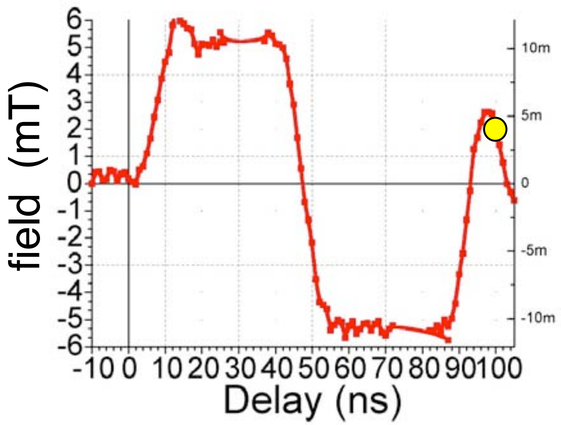

Fe

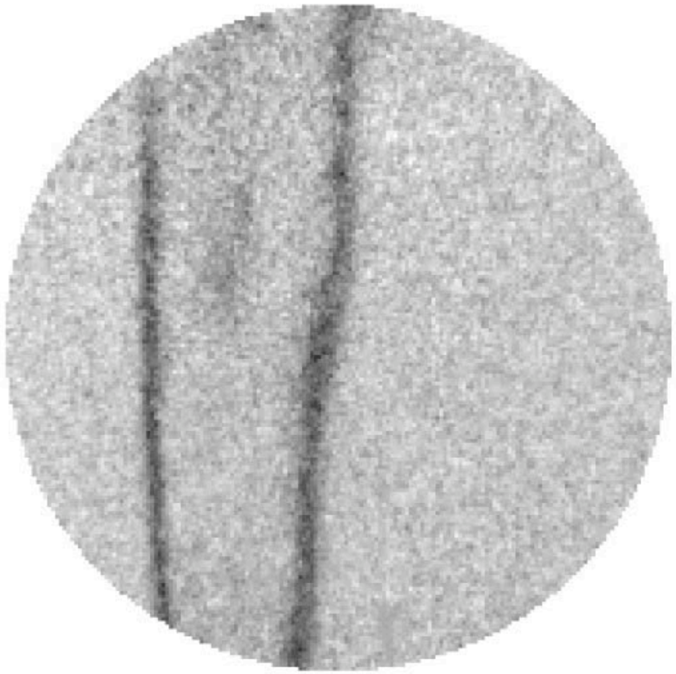

20 □m

tunnel junction

4 nm $Fe_{19}Ni_{81}$
2.5 nm Al_2O_3
7 nm Co

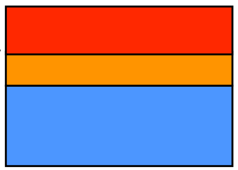

Aberration correction in light optics

DICTIONARY OF PHOTOGRAPHY
1889, London
by E.J. Wall

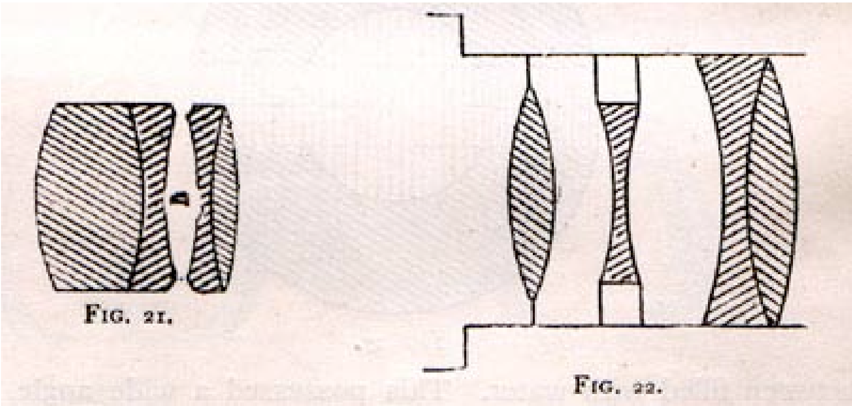

FIG. 21. FIG. 22.

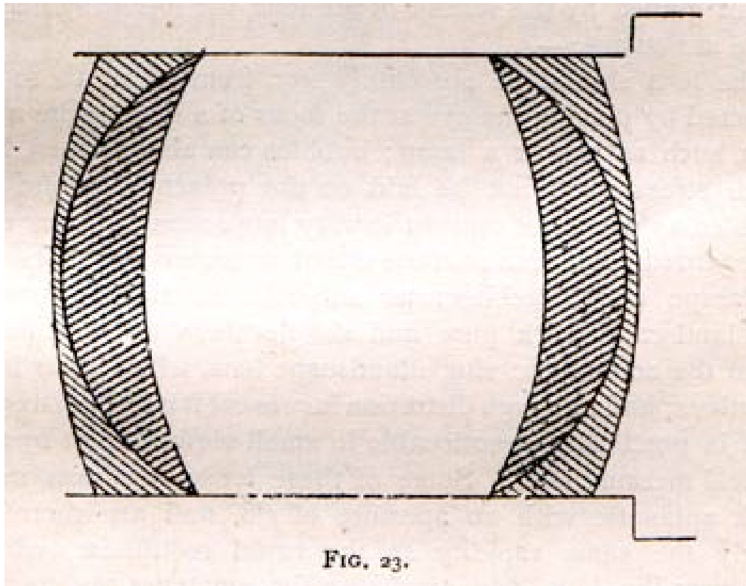

FIG. 23.

"... some of the finest lenses of the day; and in figs. 21 and 22 are shown two more of Steinheil's lenses, which work at f/2.5, No. 21 being for groups, No. 22 for portraits."

"In fig. 23 I am enabled, by the kindness of Messrs. Perken, Son, & Rayment, to give a sketch of the Euryscope lens, which is composed of two symmetrical combinations of flint glass, and works at an aperture of f/6, a great gain for rapid work. These lenses are perfectly free from spherical and chromatic aberration..."

Aberration correction in electron optics

Sphärische und chromatische Korrektur von Elektronen-Linsen.

Von O. Scherzer, z. Zt. USA.

(Aus den Süddeutschen Laboratorien in Mosbach.)

(Mit 7 Textabbildungen.)

Die Brauchbarkeit des Elektronenmikroskops bei hohen Vergrößerungen wird durch den Öffnungsfehler und die chromatische Aberration beeinträchtigt. Beide Fehler sind unvermeidlich, solange die abbildenden Felder rotations-symmetrisch, ladungsfrei und zeitlich konstant sind. Die vorliegende Untersuchung soll zeigen, daß die Aufhebung irgendeiner dieser drei Einschränkungen genügt, um den Weg zur sphärischen und chromatischen Korrektur und damit zu einer erheblichen Steigerung des Auflösungsvermögens freizugeben.

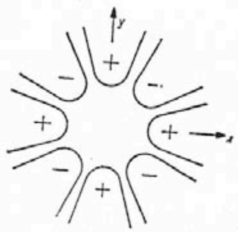

Abb. 3. Elektroden zur Erzeugung eines Feldes mit vierzähliger Symmetrie.

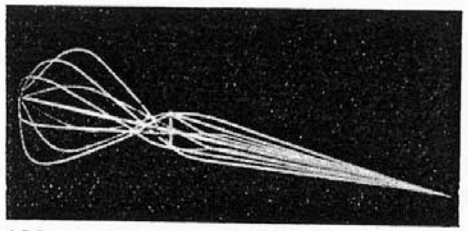

Abb. 4. Drahtmodell eines Strahlenganges mit astigmatischem Zwischenbild.

O. Scherzer, Optik 2 (1947) 114

Aberration correction by electrostatic mirror

Round convex lenses | electrostatic mirror

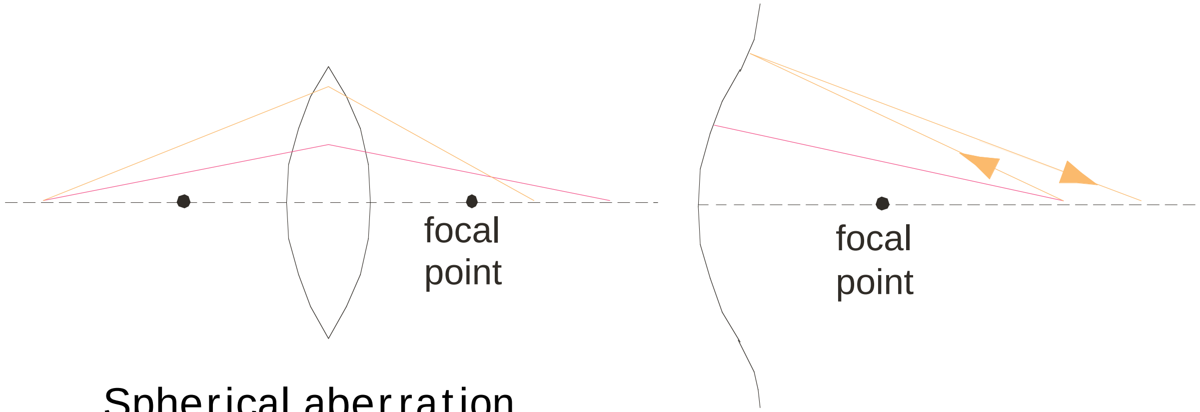

Spherical aberration

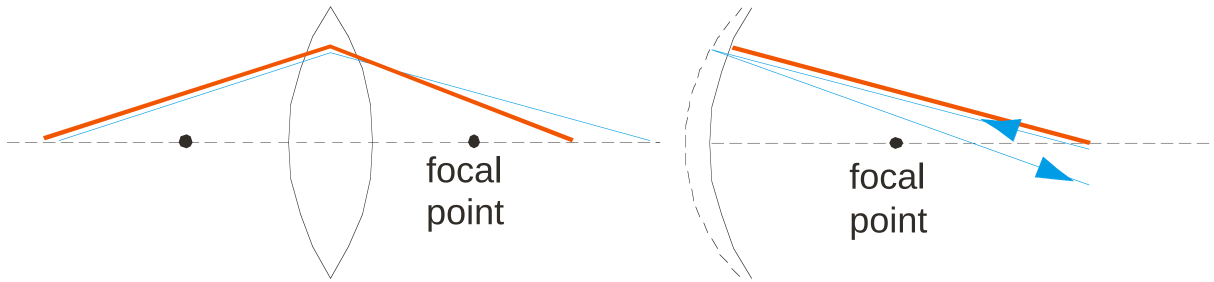

Chromatic aberration

Equipotential surfaces
in a diode mirror

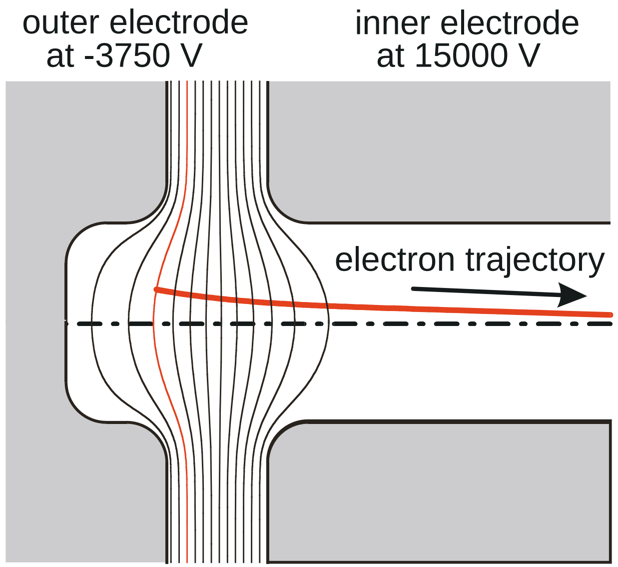

H. Rose and D. Preikszas, Nucl. Instr. & Meth. A 363 (1995) 201
R. Fink et al., JES 84 (1997) 231

LEEM/ PEEM: improved resolution by aberration correction

"SMART" project

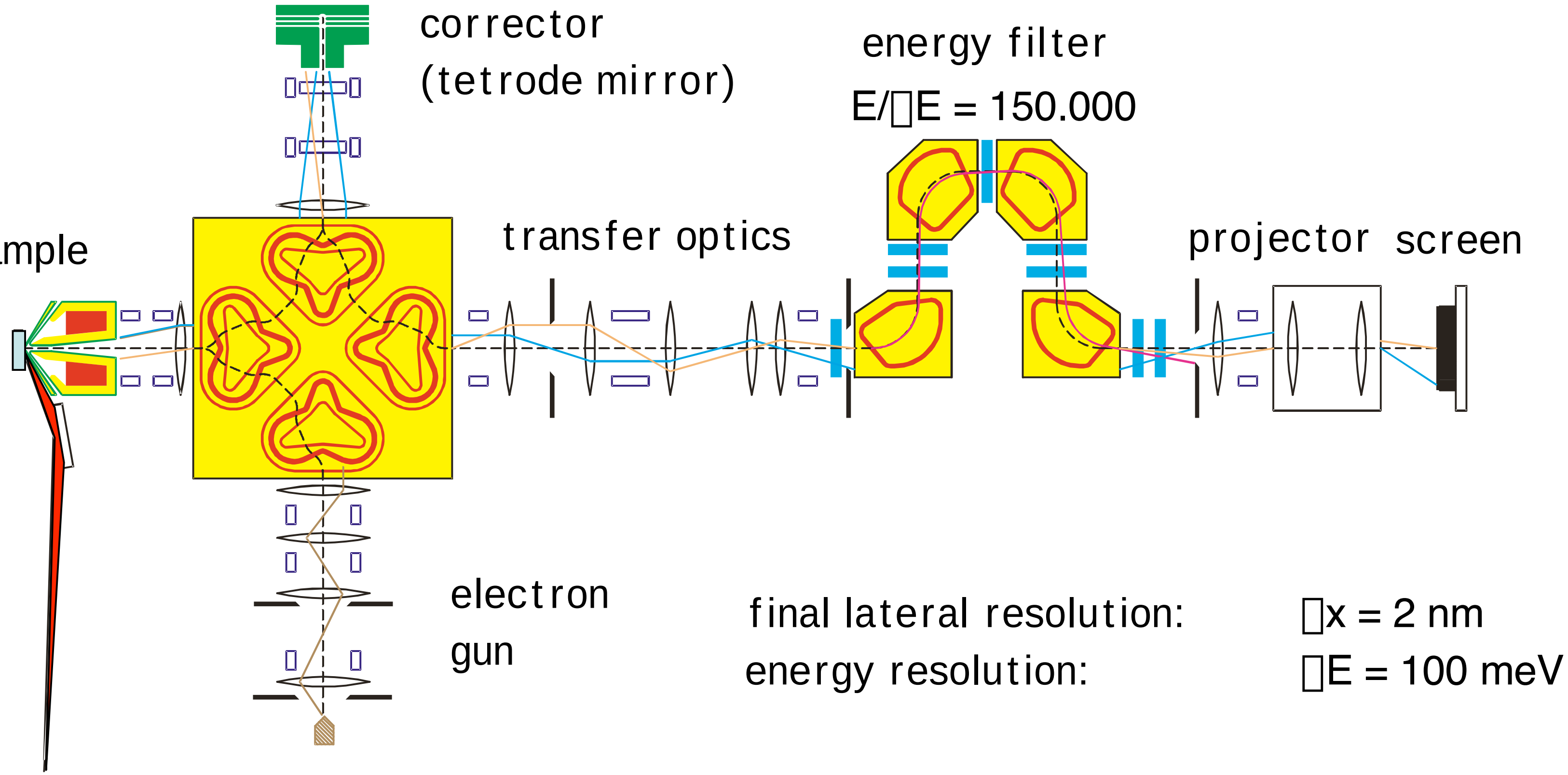

H. Rose and D. Preikszas, Nucl. Instr. & Meth. A 363 (1995) 201
R. Fink et al., JES 84 (1997) 231

“SMART” project: set-up at BESSY

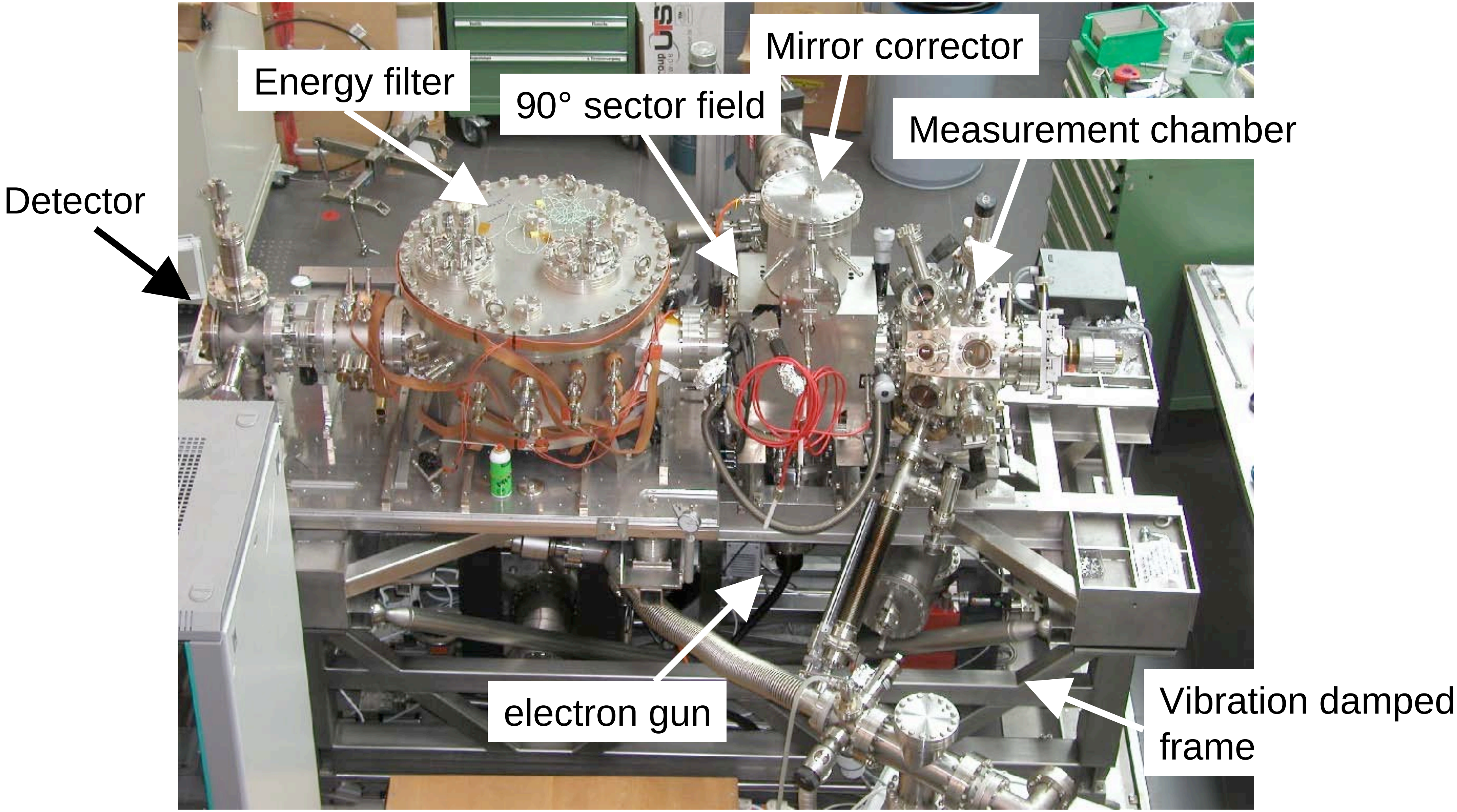

LEEM/PEEM: improved resolution by aberration correction

"SMART" target parameters:

Resolution limit	without correction	with correction
Spherical aberr.	α^3 + ...	α^5
Chromatic aberr.	$\Delta E\ \alpha$ + ...	$\Delta E\ \alpha^2$ + $\Delta E^2\ \alpha$
Diffraction	$1/\alpha$	$1/\alpha$

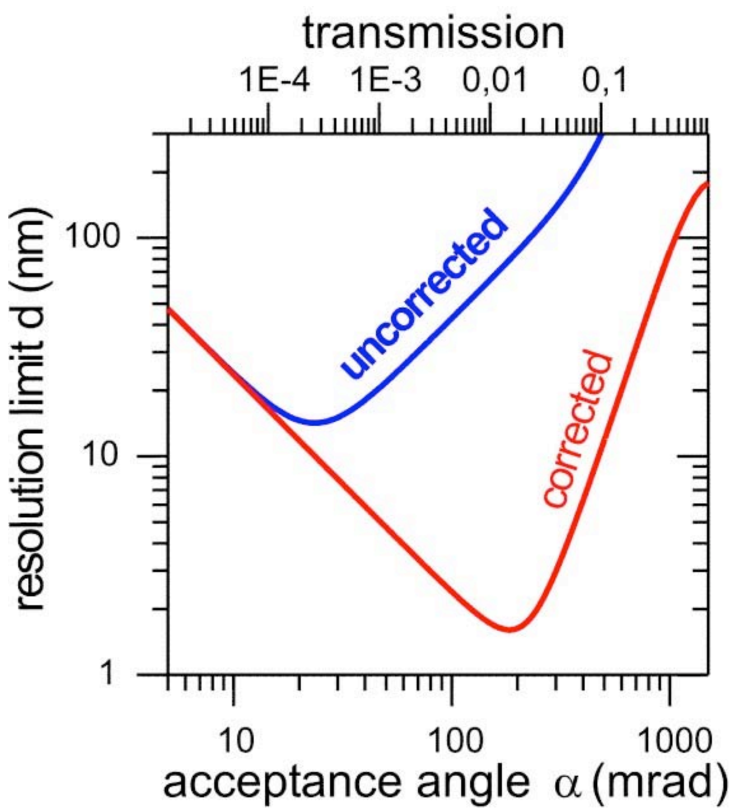

D. Preikszas and H. Rose, J. Electr. Micr. 1 (1997) 1

Th. Schmidt et al., Surf. Rev. Lett 9 (2002) 223

Coherent x-ray diffraction (speckles)

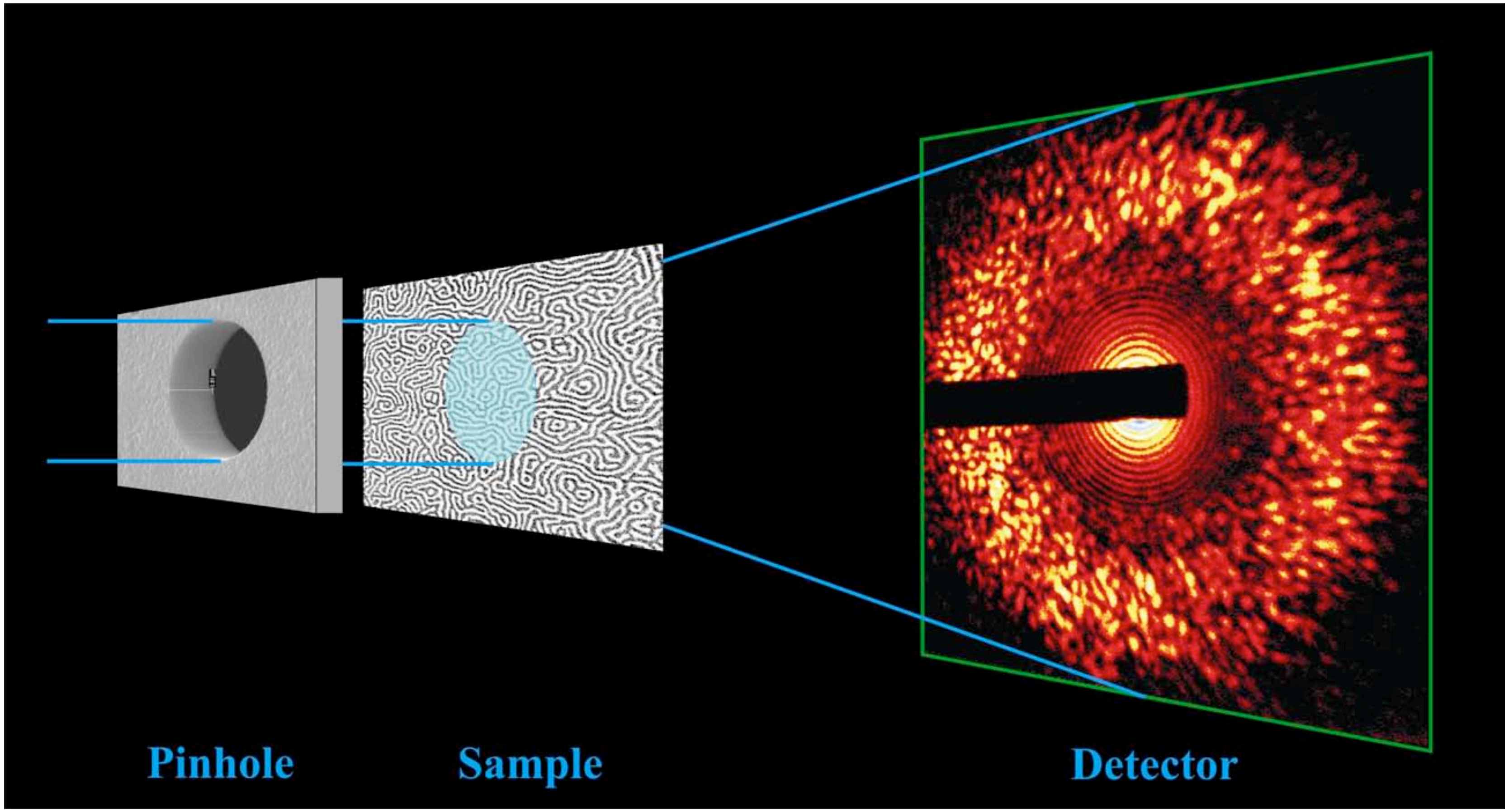

Lensless domain imaging using coherent soft x-rays

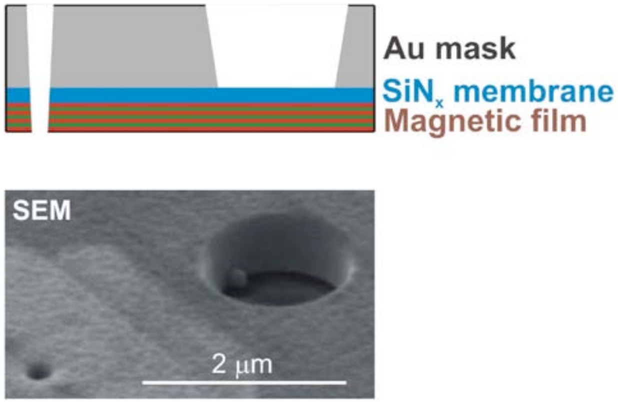

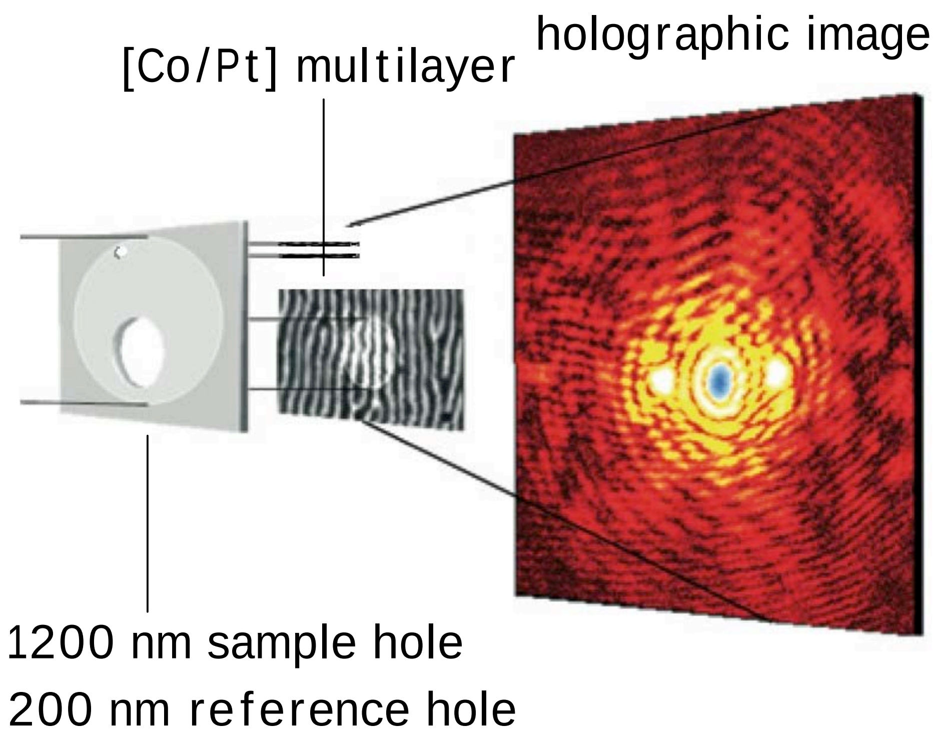

M. Lörgen et al., BESSY-Highlights 2003, p. 32

X-ray holography: Digital image reconstruction

Difference (RCP – LCP)

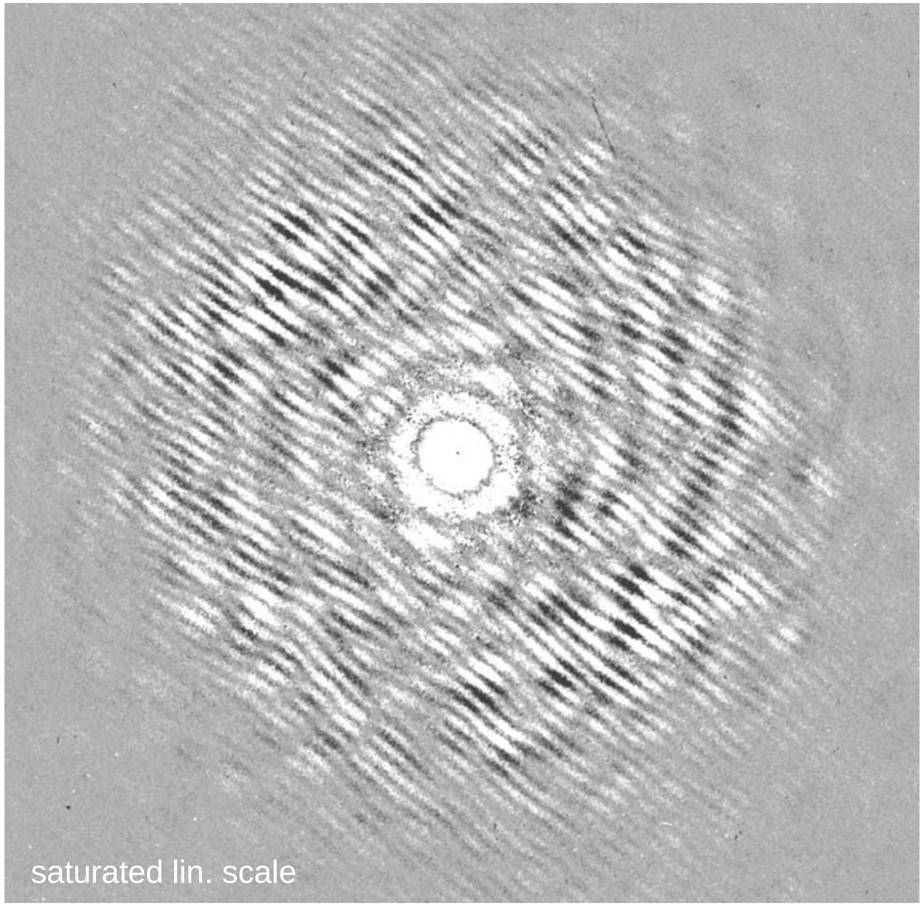

FFT (Difference)

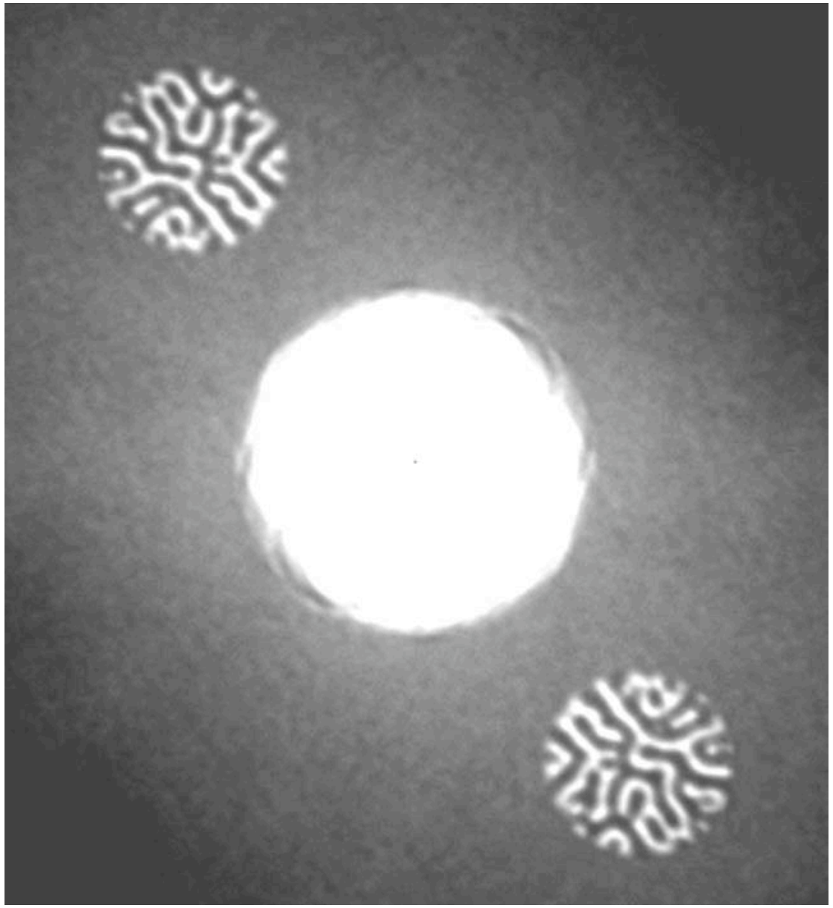

Convolution theorem applied to diffraction: FT(diffraction) = Autocorrelation (Object)

Image reconstruction from speckle hologram

FT hologram

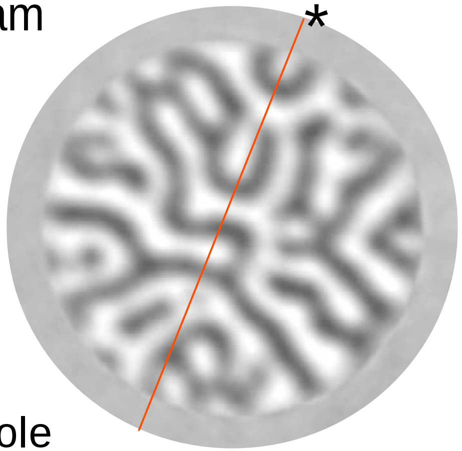

STXM image

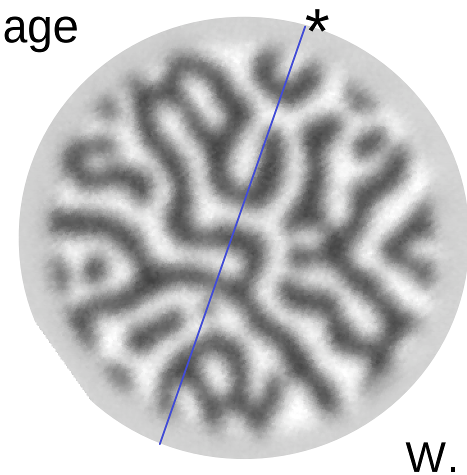

Reference hole
∅ 100 nm

W. F. Schlotter
Y. Acremann

Resolution
30 - 40 nm

[Co(4 Å)/Pt (7Å)]$_{50}$

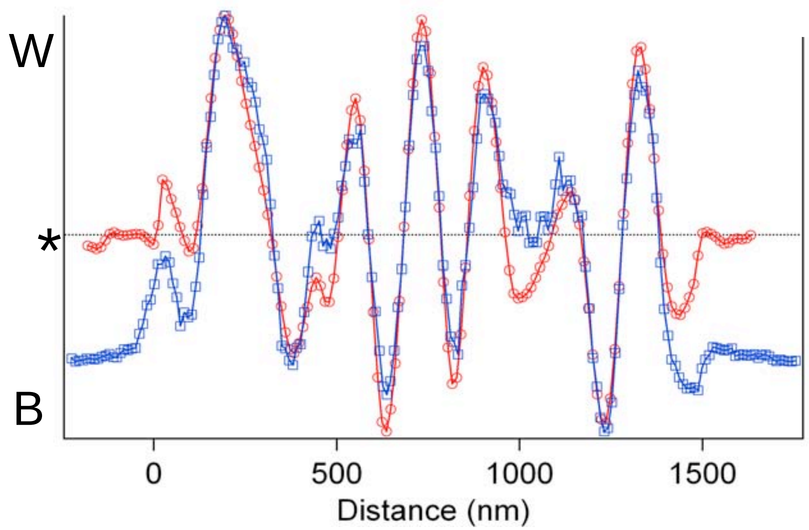

S. Eisebitt et al., Nature 432 (2004) 885

Free electron laser (FEL)

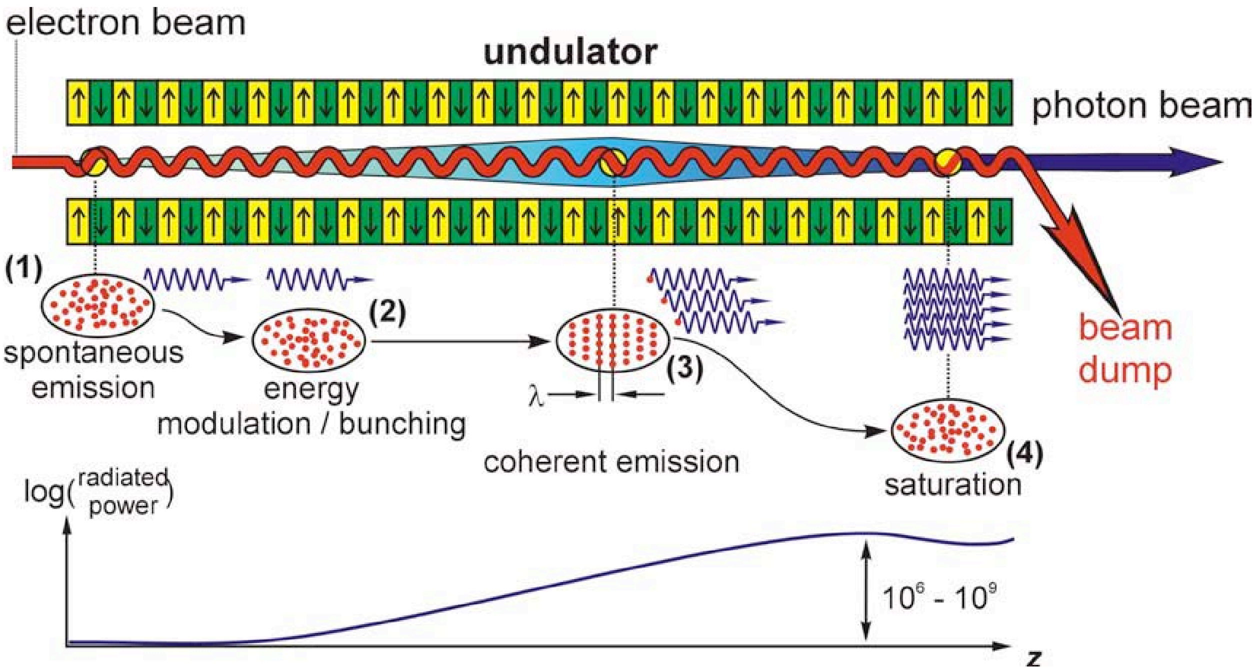

dipole bend: µ N

wiggler: µ nN

undulator: µ n^2N

FEL: µ n^2N^2

N - number of electrons

n - number of undulations

FEL performance

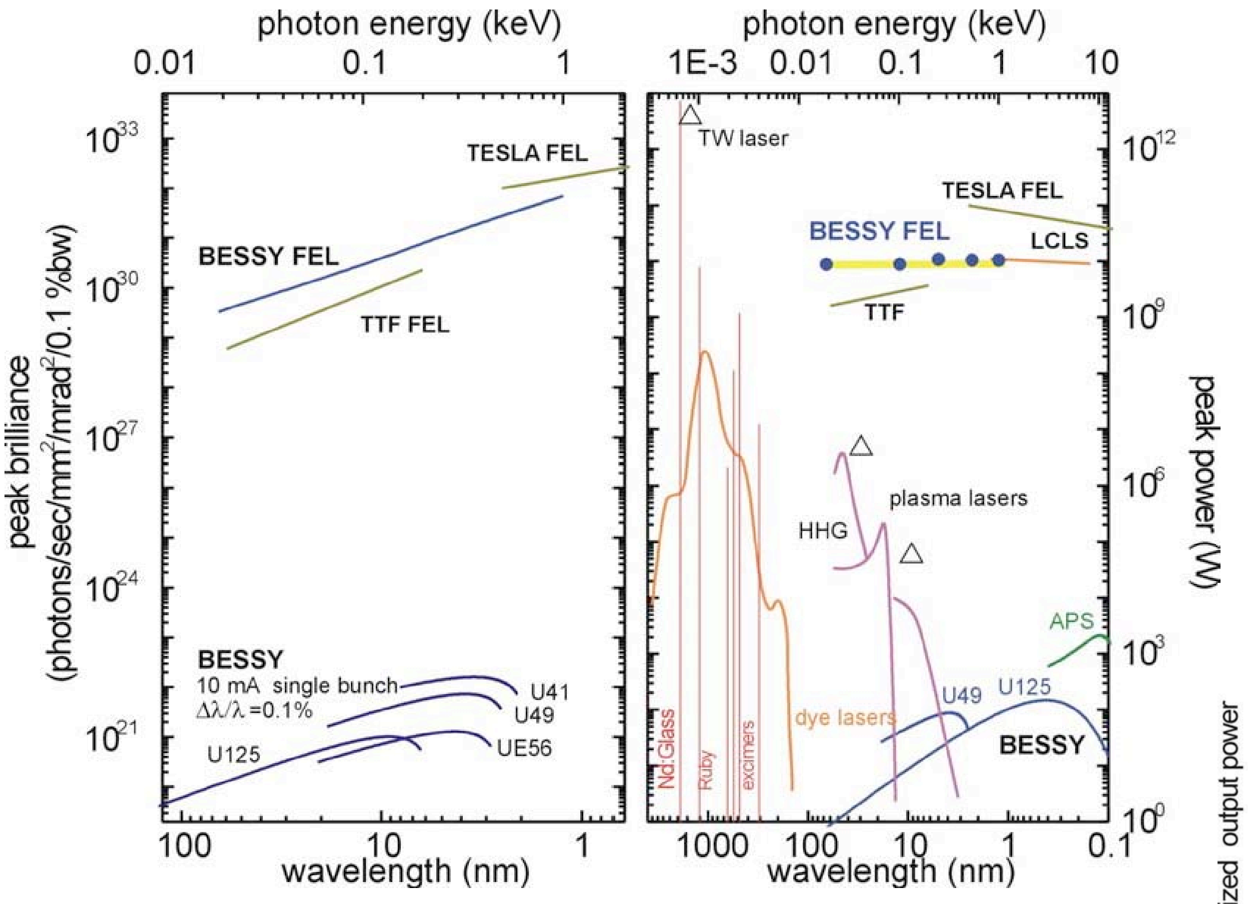

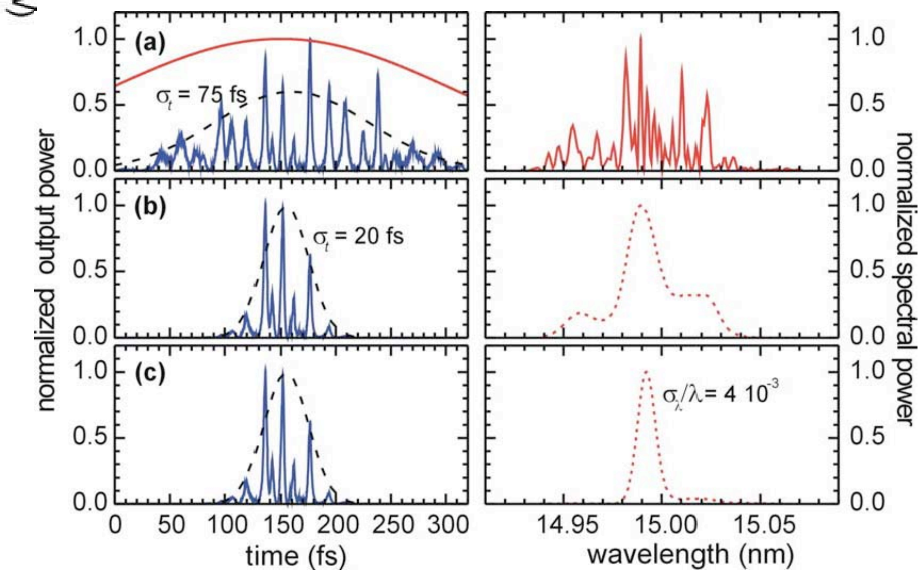

FEL project at BESSY

Exploring the nano- and femtoworld